

AFFDL-TR-77-37

2

(2)

AD A 053588

**DIGITAL SIMULATION OF FLEXIBLE AIRCRAFT
RESPONSE TO SYMMETRICAL AND ASYMMETRICAL
RUNWAY ROUGHNESS**

Anthony G. Gerardi

Structural Integrity Branch
Structural Mechanics Division

August 1977

TECHNICAL REPORT AFFDL-TR-77-37

DDC FILE COPY

Approved for public release; distribution unlimited.

AIR FORCE FLIGHT DYNAMICS LABORATORY
AIR FORCE WRIGHT AERONAUTICAL LABORATORIES
AIR FORCE SYSTEMS COMMAND
WRIGHT-PATTERSON AIR FORCE BASE, OHIO 45433

DDC
RECEIVED
MAY 3 1978
B
HL

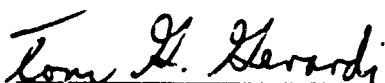
**Best
Available
Copy**

NOTICE

When Government drawings, specifications, or other data are used for any purpose other than in connection with a definitely related Government procurement operation, the United States Government thereby incurs no responsibility nor any obligation whatsoever; and the fact that the government may have formulated, furnished, or in any way supplied the said drawings, specifications, or other data, is not to be regarded by implication or otherwise as in any manner licensing the holder or any other person or corporation, or conveying any rights or permission to manufacture, use, or sell any patented invention that may in any way be related thereto.

This report has been reviewed by the Information Office (IO) and is releasable to the National Technical Information Service (NTIS). At NTIS, it will be available to the general public, including foreign nations.

This technical report has been reviewed and is approved for publication.

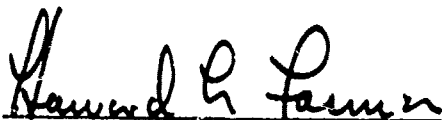


TONY G. GERARDI
Project Engineer

FOR THE COMMANDER



ROBERT M. BADER, Chief
Structural Integrity Branch
Structural Mechanics Division



HOWARD L. FARMER, COL, USAF
Chief, Structural Mechanics Division

Copies of this report should not be returned unless return is required by security considerations, contractual obligations, or notice on a specific document.

UNCLASSIFIED

SECURITY CLASSIFICATION OF THIS PAGE (When Data Entered)

REPORT DOCUMENTATION PAGE		READ INSTRUCTIONS BEFORE COMPLETING FORM
1. REPORT NUMBER AFFDL-TR-77-37	2. GOVT ACCESSION NO.	3. REPORT TYPE AND DATES COVERED Final Technical Report Sept 1975 - Aug 1976
4. TITLE (and Subtitle) DIGITAL SIMULATION OF FLEXIBLE AIRCRAFT RESPONSE TO SYMMETRICAL AND ASYMMETRICAL RUNWAY ROUGHNESS	5. PERFORMING ORGANIZATION NAME AND ADDRESS Air Force Flight Dynamics Laboratory Structural Integrity Branch Wright-Patterson AFB, Ohio 45433	6. CONTRACT OR GRANT NUMBER(s) Project No. 1367 Task No. 136701 Work Unit No. 13670113
7. AUTHOR Anthony G. Gerardi	8. CONTROLLING OFFICE NAME AND ADDRESS Air Force Flight Dynamics Laboratory Air Force Systems Command Wright-Patterson AFB, Ohio 45433	9. NUMBER OF PAGES 83
10. MONITORING AGENCY NAME & ADDRESS (if different from Controlling Office)	11. SECURITY CLASS (of Report) UNCLASSIFIED	12. DECLASSIFICATION/DOWNGRADING SCHEDULE
13. DISTRIBUTION STATEMENT (of this Report) Approved for public release; distribution unlimited		
14. DISTRIBUTION STATEMENT (of the abstract entered in Block 20, if different from Report)		
15. SUPPLEMENTARY NOTES		
16. KEY WORDS (Continue on reverse side if necessary and identify by block number) Aircraft Dynamics Simulation Ground Loads Taxi Analysis		
17. ABSTRACT (Continue on reverse side if necessary and identify by block number) A method has been developed for determining the dynamic response of a flexible aircraft to runway roughness during takeoff or constant speed taxi. The equations that formulate the mathematical model have been programmed for a CDC 6600 digital computer and uses a Calcomp plotter for part of the program output. Three sets of runway elevation data are input to provide a forcing function at each landing gear. Three runway profiles measured at Washington National Airport, runway 36, were used to represent a typical commercial (OVER)		

DD FORM 1 JAN 73 1473 EDITION OF 1 NOV 68 COMPLETE

UNCLASSIFIED

SECURITY CLASSIFICATION OF THIS PAGE (When Data Entered)

1012070

101

UNCLASSIFIED

SECURITY CLASSIFICATION OF THIS PAGE (When Data Entered)

Block No. 20 - Continued

asymmetric profile. Three lines of profile were analytically generated to represent traversing a 1-cos dip at a 45 degree angle of approach.

Several aircraft have been simulated with this program, each during a takeoff and a constant speed taxi. The data used to simulate the airplanes (McDonnell Douglas C-9A, Boeing 727-100, and an AMST) and the runway profile data used, are included in the appendix of this paper.

Comparison of simulated results to limited experimental data was good. Peak vertical acceleration levels at the pilot's station were within 14%.

The effect of the asymmetry of a profile on pilot's station vertical acceleration was significant providing the asymmetry of the profile was significant.

UNCLASSIFIED

SECURITY CLASSIFICATION OF THIS PAGE (When Data Entered)

FOREWORD

This report was prepared by A. G. Gerardi, Aerospace Engineer in the Loads and Response Prediction Group of the Structural Mechanics Division of the Air Force Flight Dynamics Laboratory at Wright-Patterson Air Force Base, Ohio. The work described herein is a part of the Air Force Systems Command exploratory development program to predict aircraft dynamic loads during ground operations. The work was directed under Project 1367, "Structural Integrity for Military Aerospace Vehicles," Task 136701, "Structural Flight Loads Data."

This report covers work done in the period from September 1975 to August 1976.

ACCESSION for		
NTIS	White Section	<input checked="" type="checkbox"/>
DOC	Buff Section	<input type="checkbox"/>
UNANNOUNCED		<input type="checkbox"/>
JUSTIFICATION _____		
BY _____		
DISTRIBUTION/AVAILABILITY CODES		
Dist.	AVAIL.	and/or SPECIAL
A		

TABLE OF CONTENTS

Section	Page
I INTRODUCTION	1
1. Purpose of the Study	1
II MATHEMATICAL MODEL	3
1. General Airplane/Runway Model	3
2. Rigid Body Equations of Motion	6
3. Flexibility Equations of Motion	7
4. Solution Technique	7
III COMPUTER PROGRAM	9
1. Output Format	9
IV DISCUSSION OF SIMULATIONS	20
V SUMMARY AND CONCLUSIONS	38
APPENDIX	
A DEVELOPMENT OF EQUATIONS OF MOTION	41
B LISTING OF COMPUTER PROGRAM TAX2	48
C LISTING OF AIRPLANE DATA	62
D LISTING OF RUNWAY PROFILE DATA	71
BIBLIOGRAPHY	74
REFERENCES	75

LIST OF ILLUSTRATIONS

Figure		Page
1.	Accepted Military Human Tolerance Vertical Vibration Criterion	2
2.	Typical Single Acting Oleo Pneumatic Landing Gear Strut	4
3.	Source Deck Setup	16
4.	Typical Calcomp Plotted Output	18
5.	Boeing 727-100 Constant Speed Taxi Simulation over the Washington National Profile Without a Roll Degree of Freedom	22
6.	Boeing 727-100 Constant Speed Taxi Simulation over the Washington National Profile With a Roll Degree of Freedom	23
7.	PSD of Washington National Airport Runway 36	24
8.	Boeing 727-100 Traversing a (1-cos) dip head-on	25
9.	Boeing 727-100 Traversing a (1-cos) dip at a 45° angle	26
10.	C-9A Traversing a (1-cos) dip at a 45° angle	28
11.	AMST Traversing a (1-cos) dip at a 45° angle	29
12.	Boeing 727-100 Taking Off from Washington National Airport With the Roll Degree of Freedom Included	30
13.	AMST Taking Off from Washington National Airport With the Roll Degree of Freedom Included	31
14.	C-9A Taking Off from Washington National Airport With the Roll Degree of Freedom Included	32
15.	PSD of Washington National Runway 36 and two Typically Smooth Runways	33
16.	Measured Response of a Boeing 727-100 Takeoff at Washington National Airport Runway 36	34
17.	C-9A with Flexible Wings Taxiing over a (1-cos) dip at a 45° angle	36

LIST OF ILLUSTRATIONS (Continued)

Figure		Page
18.	C-9A with Flexible Wings Taking Off from Washington National Runway 36	37
A-1.	Description of Asymmetrical Mathematical Model	42
C-1.	Three View of Boeing 727-100	63
C-2.	Three View of McDonnell-Douglas C-9A	66
D-1.	Washington National Runway 36 with Linear Trend Removed	72

LIST OF TABLES

Table		Page
1	Description of Input Aircraft Data	10
2	Typical Computer Output Listing	17
3	Summary of Simulations	21
	Comparisons of Simulated and Experimental Data	35

SECTION I INTRODUCTION

A common problem that can occur during takeoff and taxiing operations of aircraft is high acceleration levels caused by a rough runway. Due to these accelerations, runway must be evaluated with respect to roughness in order to ensure timely pavement maintenance to control aircraft structural loads and fatigue. Also, rough runways adversely affect the ability of the crew members by reducing instrument readability and crew comfort. Figure 1 shows the current criterion (Reference 1) used to set maximum allowable vertical acceleration levels from a human comfort standpoint. Reference 2 addressed the runway roughness problem at considerable length and contains the development of a mathematical model and subsequent computer program called "TAXI" to simulate the dynamic response of military aircraft to runway roughness on a symmetrical runway. For a symmetric runway, only one runway profile is required. Normally this is sufficient for representing a paved runway. With the advent of the AMST (Advanced Medium STOL Transport) and in some cases with conventional airplanes operating off of semiprepared or very rough paved surfaces, the rolling motion of an aircraft became significant. This rolling motion was the result of operating the aircraft on an asymmetric runway. Therefore, in order to properly simulate this response it became necessary to include the runway profile encountered by each landing gear.

1. PURPOSE OF THIS STUDY

The purpose of this study is to develop a computer program, capable of simulating an aircraft during constant speed taxi or takeoff from runways that are asymmetrical.

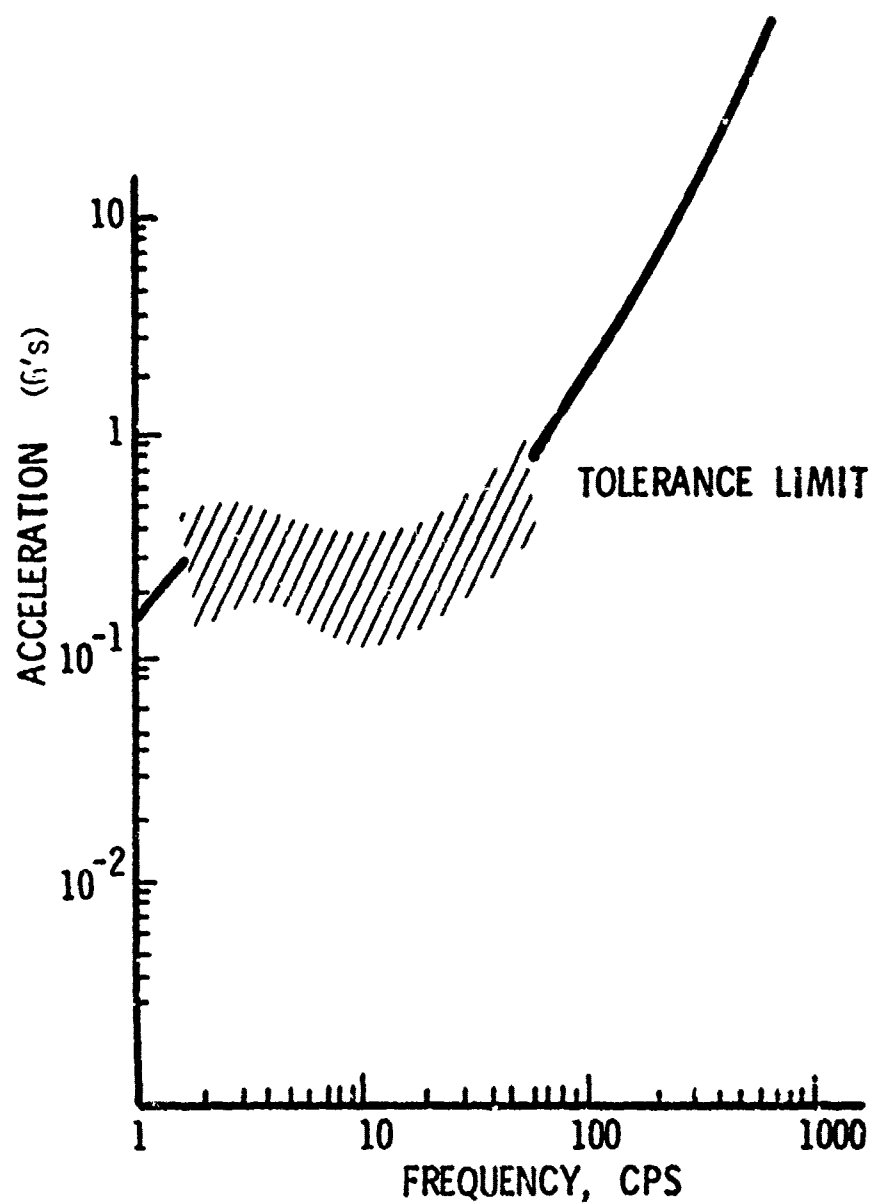


Figure 1. Accepted Military Human Tolerance Vertical Vibration Criterion

SECTION II MATHEMATICAL MODEL

The airplane/runway mathematical model used for this study was the basic mathematical model developed in Reference 2. A detailed description of the components that make up this general model, as well as the assumptions made are shown in Reference 2. This report presents, in summary form, the landing gear strut and tire representation, the airplane rigid body and flexible body representation, the runway profile representation, the equations of motion, and the solution technique.

1. GENERAL AIRPLANE/RUNWAY MODEL

The general model represents an asymmetrical body with a nose gear and a right and left main landing gear. Each landing gear strut is assumed to have point contact with the profile and it is assumed that each landing gear traverses a different profile. Aerodynamic lift and drag are modeled, and thrust is applied at the aircraft's center of gravity.

The airplane is free to roll, pitch, plunge, and translate horizontally down the runway and each landing gear unsprung mass is free to translate vertically. To these rigid body degrees of freedom, up to 30 flexible modes of vibration are included. This airplane motion is controlled by the landing gear strut forces, lift, drag, thrust, and the resisting parameters of aircraft mass and inertia.

The landing gear struts are nonlinear, single acting oleo pneumatic energy absorbing devices (Figure 2) and are represented in the model as the sum of the three forces; pneumatic, hydraulic, and strut bearing friction forces. The pneumatic force, which is the largest of the three is represented by the equation:

$$F_A = \frac{PV}{\frac{V}{A} - S} \quad (1)$$

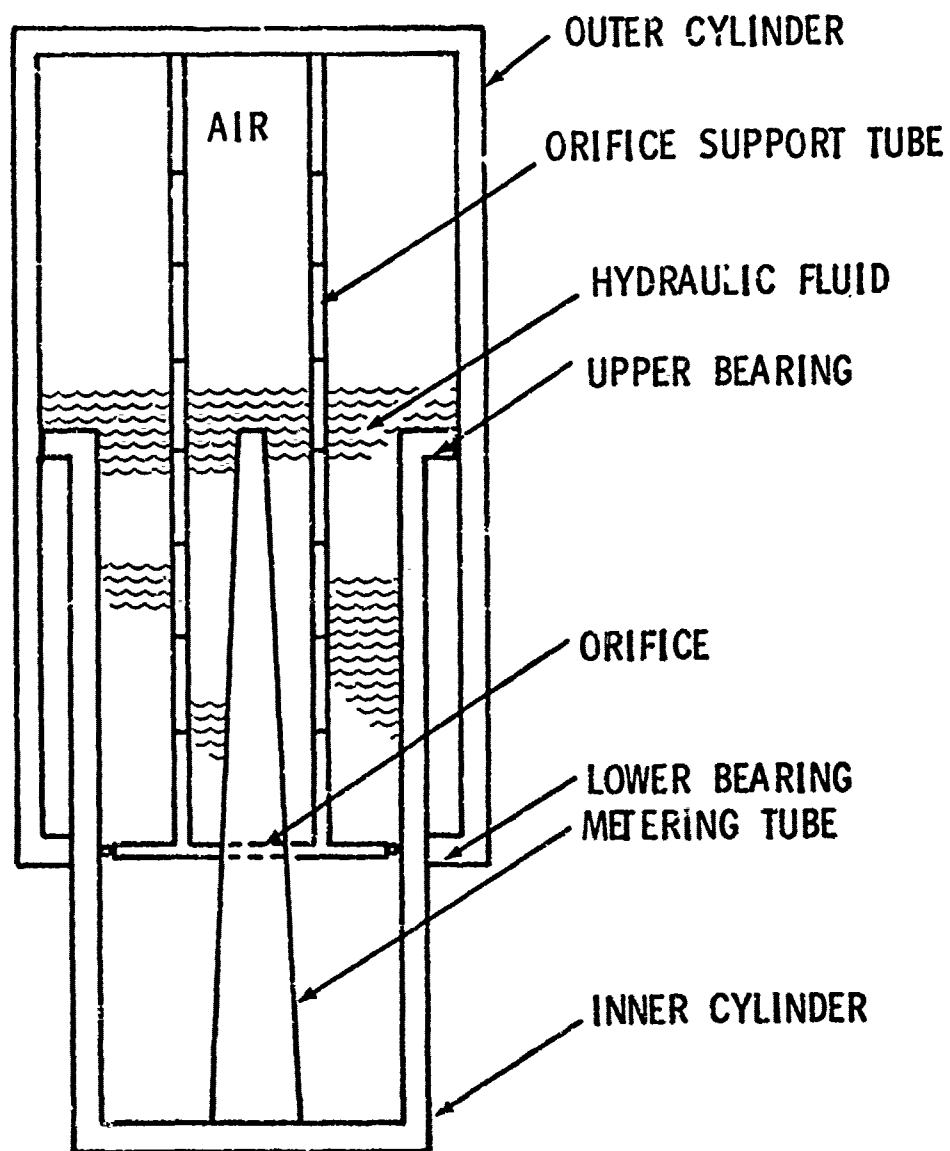


Figure 2. Typical Single Acting Oleo Pneumatic Landing Gear Strut

where:

P = fully extended strut pressure
 V = fully extended strut volume
 A = pneumatic piston area
 S = strut stroke

The damping force is given by the equation:

$$F_h = \frac{\rho_h A_h^3 \dot{S} |\dot{S}|}{2 (C_d A_o)^2} \quad (2)$$

where:

ρ_h = density of the hydraulic fluid
 A_h = the hydraulic piston area
 A_o = effective orifice area (constant orifice minus metering pin area)
 C_d = orifice coefficient (use 0.9)
 \dot{S} = strut piston velocity

The third strut force is the strut bearing friction force and is neglected in the model because the force is small for symmetrically loaded struts. (See Reference 2).

The tire force is represented by the linear equation:

$$F_T = k T_D \quad (3)$$

where:

T_D = tire deflection
 k = linear tire spring constant

The runway elevation data is input into the model in two foot increments. The profile is made continuous by fitting the following

polynomial through the three elevation data points and the slope at the end of the previous profile segment:

$$y(x) = a_1 + a_2x + a_3x^2 + a_4x^3 \quad (4)$$

where:

$a_{1,2,3,4}$ = coefficients derived from the elevation and slope data

This is done for each of the three lines of runway profile data.

2. RIGID BODY EQUATIONS OF MOTION

The differential equations of motion for the mathematical model were derived by application of the Lagrange equations (See Appendix A). The general form of these equations is shown below and corresponds to the notation shown in Figure A-1 in Appendix A.

$$\ddot{Z} = (F_{s1*} + F_{s2} + F_{s3} + L - W)/M_{cg} \quad [\text{c.g., vertical acceleration}] \quad (5)$$

$$\ddot{Z}_1 = (F_{t1} - F_{s1} - W_1)/M_1 \quad [\text{unsprung mass vertical acceleration}] \quad (6)$$

$$\ddot{Z}_2 = (F_{t2} - F_{s2} - W_2)/M_2 \quad [\text{unsprung mass vertical acceleration}] \quad (7)$$

$$\ddot{Z}_3 = (F_{t3} - F_{s3} - W_3)/M_3 \quad [\text{unsprung mass vertical acceleration}] \quad (8)$$

$$\ddot{\theta} = (F_{s1}^A + F_{s2}^B + F_{TD}^C - F_{s3}^C)/I_{yy} \quad [\text{pitching acceleration}] \quad (9)$$

$$\ddot{\phi} = (F_{s3} - F_{s2})C/I_{xx} \quad [\text{rolling acceleration}] \quad (10)$$

$$\ddot{X} = (F_T - F_{TD} - F_{AD})/(M_{cg}) \quad [\text{horizontal translation acceleration}] \quad (11)$$

where:

F_{s1}, F_{s2}, F_{s3} = total landing gear strut forces

F_{t1}, F_{t2}, F_{t3} = tire forces

$M_{cg}, W, I_{yy}, I_{xx}$ = aircraft mass, weight, and pitching and roll inertias

*The subscript 1, 2 and 3 corresponds to the nose, right main and left main landing gears respectively.

W_1, W_2, W_3 = upsprung landing gear weights
 A, B, C, ϵ_1 = moment arms
 L, F_T, F_{TD}, F_{AD} = lift, thrust, and tire and aerodynamic drag forces
 $[F_T \text{ and } F_{AD} \text{ act through the center of gravity}]$

3. FLEXIBILITY EQUATIONS OF MOTION

$$M_i \ddot{q}_i = \epsilon_{i1} F_{s1} + \epsilon_{i2} F_{s2} + \epsilon_{i3} F_{s3} - 2\zeta_i \omega_i \dot{q}_i - \omega_i^2 M_i q_i \text{ for the } i\text{th mode}$$

where:

M_i = the generalized mass
 $\epsilon_{i1}, \epsilon_{i2}, \epsilon_{i3}$ = modal deflections at gear location 1, 2 and 3
 ω_i = modal frequency
 ζ = damping factor
 $q_i = \dot{q}_i, \ddot{q}_i$ = generalized coordinates and their time derivatives.

The sign convention is as follows:

Z = Vertical Displacement + up
 θ = Pitch + nose down
 ϕ = Roll + roll right
 q = Deflection Due to Bending + up
 X = Horizontal Translation + forward

4. SOLUTION TECHNIQUE

The technique used for solving the coupled nonlinear differential equations of motion that describe the simulated aircraft is a three-term Taylor series. For example, the equation:

$$\ddot{x} = -c\dot{x} - kx \quad (12)$$

The three term Taylor series representations can be written as

$$x_{(I+1)} = x_{(I)} + \dot{x}_{(I)} (\Delta t) + \ddot{x}_{(I)} \frac{(\Delta t)^2}{2} \quad (13)$$

where: $I = 1 \rightarrow N$

The values for \ddot{x} , \dot{x} and x from the previous step are substituted into Equation 13 and a new value for x is obtained. Differentiating Equation 13 we obtain for the velocity \dot{x} , the expression:

$$\dot{x}_{(I+1)} = \dot{x}_{(I)} + \ddot{x}_{(I)} (\Delta t) \quad (14)$$

The values for \dot{x} and \ddot{x} are then substituted into Equation 14 and a new value of \dot{x} is found. This entire process is repeated with the new values of x and \dot{x} to obtain the next point in the solution.

SECTION III COMPUTER PROGRAM

The computer program, TAX2, which computes the dynamic response of a flexible aircraft to an asymmetrical runway profile, consists of one basic program and several subroutines. A complete listing of the program is contained in Appendix B. Table 1 contains a description of the aircraft input data and Figure 3 shows the source deck setup for use on the CDC 6600 computer at Wright-Patterson AFB, Ohio.

1. OUTPUT FORMAT

The results of the calculations are presented as both a printed output and a time history plot. The printed output lists the value of fifteen parameters each 0.01 second. A sample of this listed output is shown in Table 2. The fifteen parameters listed in the heading are:

XMAINL	-	Left Main landing gear strut deflection (inches)
XMAINR	-	Right Main landing gear strut deflection (inches)
XNOSE	-	Nose gear strut deflection (inches)
ZPML	-	Left Main landing gear runway elevation (inches)
ZPMR	-	Right Main landing gear runway elevation (inches)
ZPN	-	Nose landing gear runway elevation (inches)
BETADD	-	Rolling acceleration (ϕ) (rad/sec ²)
THETADD	-	Pitching acceleration (θ) (rad/sec ²)
BETA	-	Roll angle (ϕ) (rad)
THETA	-	Pitch angle (θ) (rad)
SPEED	-	Aircraft velocity (ft/sec)
DISTANCE	-	Distance traveled down the runway (feet)
TIME	-	Real time (seconds)
CGACC	-	Center of Gravity Vertical Acceleration (g's)
PSA	-	Pilot's Station Vertical Acceleration (g's)

Figure 4 shows a photographic reduction of a typical Calcomp-plotted time history. This figure depicts a Boeing 727-100 taxiing at 50 fps over a 1-cos bump at a 45° angle of approach. The plotted output includes titles showing the airplane simulated, its gross weight,

TABLE 1
DESCRIPTION OF INPUT AIRCRAFT DATA
Section 1 (cards 1-5) - General Airplane Data

Card Column	Format	Variable Name	Data for McDonnell-Douglas C-9A	Definition
<u>Card 1</u>				
1-80	8A10	PLANE	McDonnell-Douglas C-9A	Airplane Being Simulated and Gross Weight
<u>Card 2</u>				
1-10	F10.1	W	108000.	Vehicle Weight (lbs)
11-20	F10.1	A	51.6	Distance Main Gear to CG (in)
21-30	F10.1	B	589.4	Distance Nose Gear to CG (in)
31-40	F10.1	MMI	20800000.	Pitch Moment of Inertia (lb in sec ²)
41-52	F12.0	WS	96.	Wing Station of Main Gear (in)
53-64	F12.0	MMIR	8000000.	Roll Moment of Inertia (lb in sec ²)
<u>Card 3</u>				
1-10	F10.2	PSARM	607.0	Distance of Pilot Station to CG (in)
11-20	F10.2	TAILRM	318.5	Distance of Tail Station to CG (in)
<u>Card 4</u>				
1-10	F10.2	SPEED	50.	Initial Velocity of Airplane (ft/sec)
11-20	F10.2	THRUST	29000.	Total Airplane Thrust (lbs)
21-30	F10.2	TAKEOFF	285.5	Airplane Rotation Speed (ft/sec)

TABLE 1 (Continued)

Card Column	Format	Variable Name	Data for McDonnell-Douglas C-9A	Definition
<u>Card 5</u>				
1-10	F10.4	CL	1.1	Lift Coefficient
11-20	F10.4	AREA	1000.7	Wing Area (ft ²)
21-30	F10.4	CD	.1	Drag Coefficient
<u>Section 2 (cards 6-11) - Main and Nose Gear</u>				
<u>Card 6</u>				
1-10	F10.2	WM	957.16	Unsprung Weight of Each Main Gear (lbs)
11-20	F10.2	WN	153.43	Unsprung Weight of Nose Gear (lbs)
21-30	F10.2	SXM	2.	Number of Main Gear Struts
31-40	F10.2	SXN	1.	Number of Nose Gear Struts
<u>Card 7</u>				
1-10	F10.5	AHN	6.745	Hydraulic Piston Area Nose (in ²)
11-20	F10.5	AAN	8.2958	Pneumatic Piston Area Nose (in ²)
21-30	F10.5	AHM	16.5	Hydraulic Piston Area Main (in ²)
31-40	F10.5	AAM	21.648	Pneumatic Piston Area Main (in ²)
<u>Card 8</u>				
1-10	F10.5	PAON	120.	Nose Strut Preload Pressure (lbs/in ²)
11-20	F10.5	PAOM	220.	Main Strut Preload Pressure (lbs/in ²)

TABLE 1 (Continued)

Card Column	Format	Variable Name	Data for McDonnell-Douglas C-9A	Definition
21-30	F10.5	VON	126.2	Fully Extended Nose Strut Air Volume (in ³)
31-40	F10.5	VOM	366.0	Fully Extended Main Strut Air Volume (in ³)
41-50	F10.5	OAM	.543	Orifice Area Main (in ²)
51-60	F10.5	OAN	.442	Orifice Area Nose (in ²)
<u>Card 9</u>				
1-10	F10.3	SLM	85.5	Distance from Axle to CG Waterline Main Gear Strut Unloaded (in)
11-20	F10.3	SLN	87.3	Distance from Axle to CG Waterline Nose Gear Strut Unloaded (in)
<u>Card 10</u>				
1-10	F10.1	TSM	23428.6	Main Tire Spring Constant Per Strut (lbs/in)
11-20	F10.1	TSN	8632.5	Nose Tire Spring Constant Per Strut (lbs/in)
<u>Card 11</u>				
1-10	F10.5	DX	.001	Integration Step Size
<u>Card 12</u>				
1-5	I5	IFPLOT	0	0-Plot; 1-No Plot
6-10	I5	IFLIST	0	0-List; 1-No List
<u>Section 3 (cards 13-16) - Metering Pin Description</u>				
<u>Card 13</u>				
1-5	I5	NSCN	5	Number of Slope Changes Nose Gear

TABLE 1 (Continued)

Card Column	Format	Variable Name	Data for McDonnell- Douglas C-9A	Definition
<u>* Card 14A, 14B,....</u>				
1-10	F10.3	STROKN (1)	*	Stroke Corresponding to Metering Pin Diameter, Nose Gear
11-20	F10.3	PINDN (1)	*	Metering Pin Diameter, Nose Gear (in)
<u>Card 15</u>				
1-5	I5	NSCM	*	Number of Slope Changes Main Gear
<u>* Card 16A, 16B,....</u>				
1-10	F10.3	STROKM (1)	*	Stroke Corresponding to Metering Pin Diameter, Nose Gear
11-20	F10.3	PINDM (1)	*	Metering Pin Diameter, Main Gear (in)
<u>Section 4 (cards 17-19) - Flexibility Data</u>				
<u>Card 17</u>				
1-5	I5	NFM	7	Number of Symmetrical Flexible Modes
6-10	I5	NAFM	7	Number of Asymmetrical Modes
<u>** Card 18A, 18B,....</u>				
1-10	F10.3	SIMAIN (1)	**	Mode Shape Deflection Main Gear
11-20	F10.3	SINOSE (1)	**	Mode Shape Deflection Nose Gear
21-30	F10.3	SICG (1)	**	Mode Shape Deflection CG
31-40	F10.3	SITAIL (1)	**	Mode Shape Deflection Tail Station

TABLE 1 (Continued)

Card Column	Format	Variable Name	Data for McDonnell-Douglas C-9A	Definition
41-50	F10.3	SIPS	**	Mode Shape Deflection Pilot Station
<u>** Card 19A, 19B,....</u>				
1-15	F15.2	GM (I)	**	Generalized Mass (lbs sec ² /in)
16-25	F10.3	OMEGA (I)	**	Modal Frequency (rad/sec)
<u>** Card 20A, 20B,....</u>				
1-10	F10.3	SILEFT (I)	**	Deflection for Left Main Gear
11-20	F10.3	SIRIGHT (I)	**	Deflection for Right Main Gear
<u>** Card 21A, 21AB,....</u>				
1-15	F15.3	GMA (I)	**	Asymmetrical Generalized Mass (lbs sec ² /in)
16-25	F10.4	OMEGAA (I)	**	Asymmetrical Modal Frequency (rad/sec)

* One card is required for each stroke-metering pin combination read into the program.

** One card is required for each flexible mode.

Note: A summary of all the data used in this study is shown in Appendix C.

TABLE 1 (Concluded)

Runway Profile Magnetic Tape

The runway profile is read into the program from a magnetic tape or permanent file. The format for this is shown below:

Column	Format	Variable Name	Definition
<u>Read 1</u>			
1-80	8A10	SITE**	Runway Profile and Direction
<u>Read 2</u>			
1-6	I6	NPTSS**	Number of Runway Elevation Points
<u>* Read 3, 4, ..., N+2</u>			
1-70	10F7.3	ELEV**	Runway Profile Data
		ELEV	
		ELEVR	

* One read required for every ten runway profile elevation points.

** The process is repeated for each of the three profiles.

Note: All of the runway profile data used in this study is listed in Appendix D.

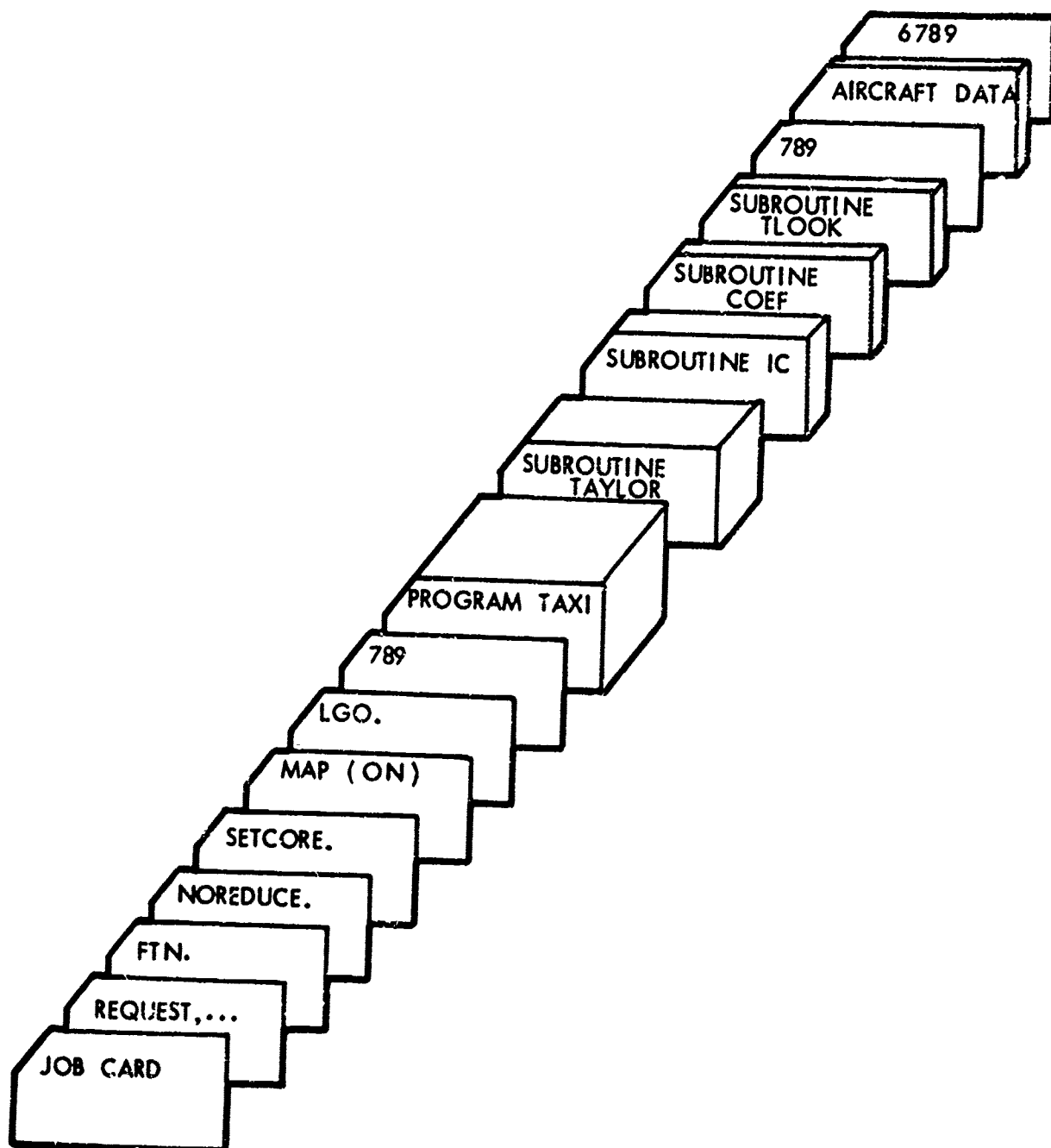


Figure 3. Source Deck Setup

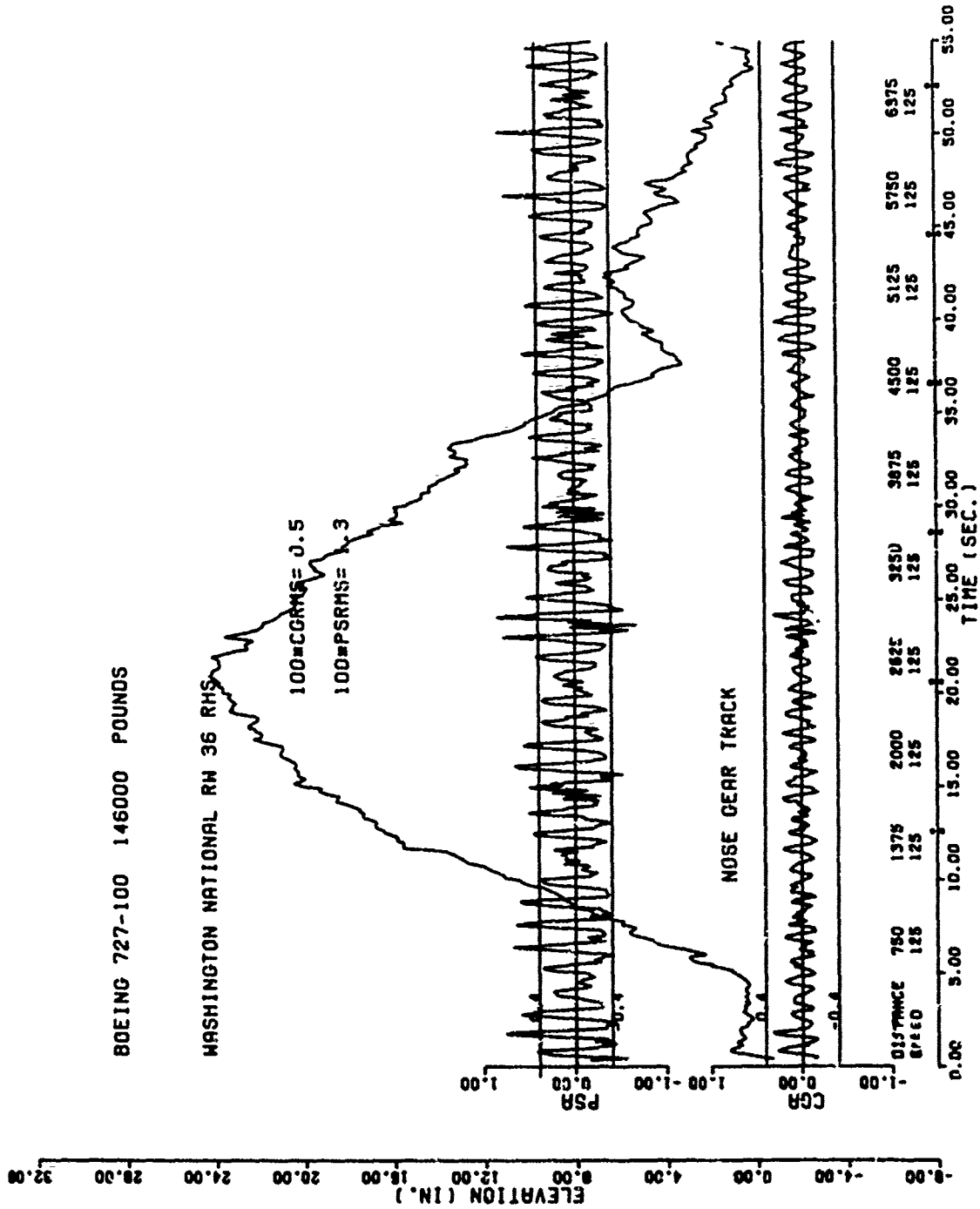


Figure 4. Typical Calcomp Plotted Output

the runway number and its location. The abscissa is the time axis annotated every second. At every time annotation the current value of aircraft speed, in feet per second, and the current aircraft position on the runway, in feet, are printed out. Runway markers (1,000-foot markers) are also plotted on the time scale to aid in aircraft positioning. The plot titled "Nose Gear Track" is a time history of the runway profile as it is encountered by the aircraft's nose gear. The actual runway profile is preceded by 100 feet of smooth surface to allow any starting transients to damp out prior to encountering the actual profile. There are two aircraft acceleration time histories that are of particular interest. One is the vertical acceleration at the pilot's station (PSA), the other is the vertical acceleration at the aircraft's center of gravity (CGA). Each time history is banded by the human tolerance criterion of ± 0.4 g. In order to minimize the amount of computer central memory required to store the acceleration time histories, the higher frequency components were effectively filtered out by limiting the sampling interval. All of the acceleration peaks, however, are shown on the plot. It should be noted that the pilot station acceleration time history is not always within the band of accepted human tolerance criteria. Thus, the plot is very useful in that it provides a graphical record of the level of acceleration, and it shows which bumps in the runway profile caused the high acceleration response.

SECTION IV DISCUSSION OF SIMULATIONS

Table 3 contains a summary of the simulations made in this study. Three different airplanes were simulated: the Boeing 727-100, the McDonnell Douglas C-9A, and an AMST configuration. Each airplane was simulated traversing two profiles: Washington National Runway 36, and a 1-cos dip. Simulations were made using mathematical models with and without a roll degree of freedom, i.e. one or three profiles, and with and without flexible wings so that comparisons of the responses could be made.

Figures 5 and 6 show the plotted results of a Boeing 727-100 traversing the Washington National runway profile without a roll degree of freedom and with a roll degree of freedom respectively. Both runs were made at a constant speed of 125 feet per second, because this speed produced higher levels of vertical acceleration for this airplane. Comparison of these two figures shows a significant increase in the vertical acceleration at the pilot's station (P.S.) while the aircraft is at different locations on the runway. For example, at T=46 sec. P.S. acceleration levels more than doubled when three lines of profile were used. This is attributed to the fact that the profiles seen by the main landing gear were rougher in the latter case. Figure 7 shows the Power Spectral Density (PSD) levels of each line of survey for the Washington National runway. A PSD is a measure of the relative roughness of a runway versus frequency. It can be seen that the PSD level is different for each line of survey which accounts for the change in the aircraft's dynamic response. Figures 8 and 9 show the 727-100 traversing a 1-cos dip headon and at a 45° angle respectively. In this case the speed was 50 fps which "tunes" the natural pitching frequency (1 cps) of the 727-100 to this 1-cos dip. Hitting the 1-cos dip at an angle caused an increase in the peak P.S. and C.G. acceleration levels.

It was necessary to try to simulate different aircraft with the computer program in an effort to check the program's versatility.

TABLE 3
SUMMARY OF SIMULATIONS

Run #	Airplane	Profile	Speed	Remarks
1	727-100	Washington National (C)	125 fps	No Roll DOF [*] , Rigid Wings
2	727-100	Washington National (L,C,R)	125 fps	With Roll DOF, Rigid Wings
3	727-100	(1-cos) (C)	50 fps	No Roll DOF, Rigid Wings
4	727-100	(1-cos) (L,C,R)	50 fps	With Roll DOF, Rigid Wings
5	C-9A	(1-cos) (L,C,R)	50 fps	With Roll DOF, Rigid Wings
6	AMST	(1-cos) (L,C,R)	50 fps	With Roll DOF, Rigid Wings
7	727-100	Washington National (L,C,R)	Takeoff	With Roll DOF, Rigid Wings
8	AMST	Washington National (L,C,R)	Takeoff	With Roll DOF, Rigid Wings
9	C-9A	Washington National (L,C,R)	Takeoff	With Roll DOF, Rigid Wings
10	C-9A	(1-cos) (L,C,R)	50 fps	With Roll DOF, Flexible Wings
11	C-9A	Washington National (L,C,R)	Takeoff	With Roll DOF, Flexible Wings

* Degree of Freedom

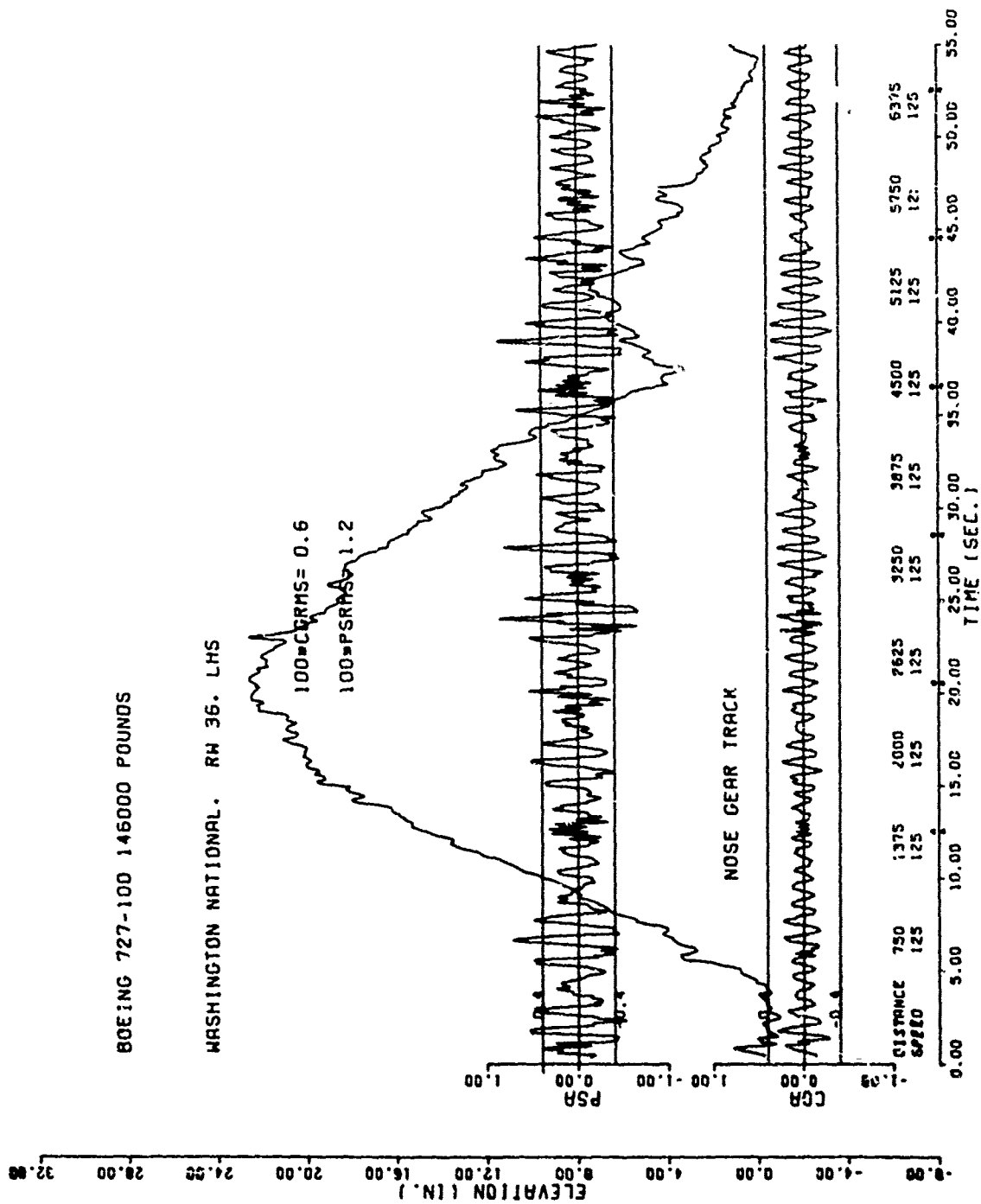


Figure 5. Boeing 727-100 Constant Speed Taxi Simulation over the Washington National Profile Without a Roll Degree of Freedom

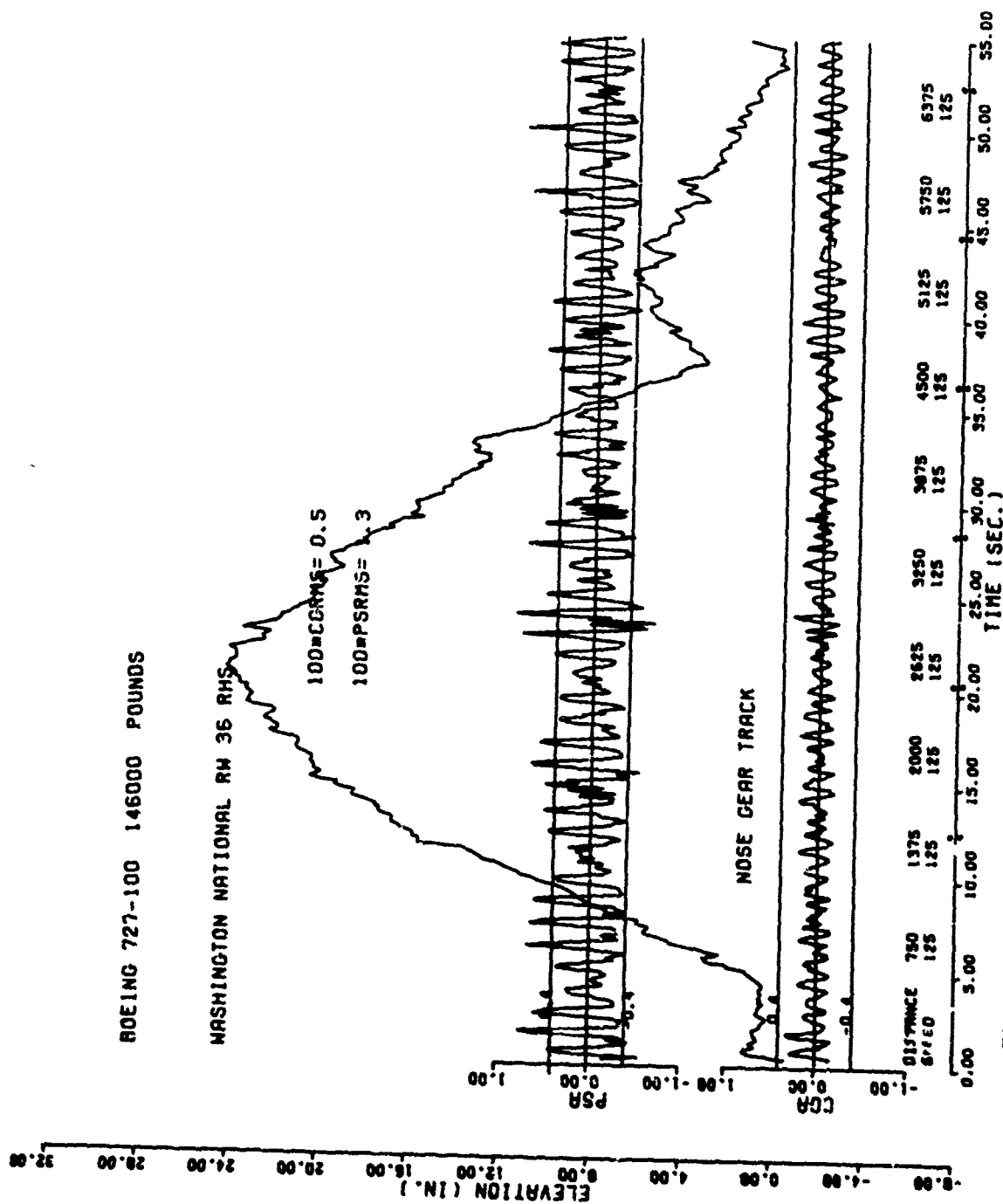


Figure 6. Boeing 727-100 Constant Speed Taxi Simulation over the Washington National Profile with a Roll Degree of Freedom

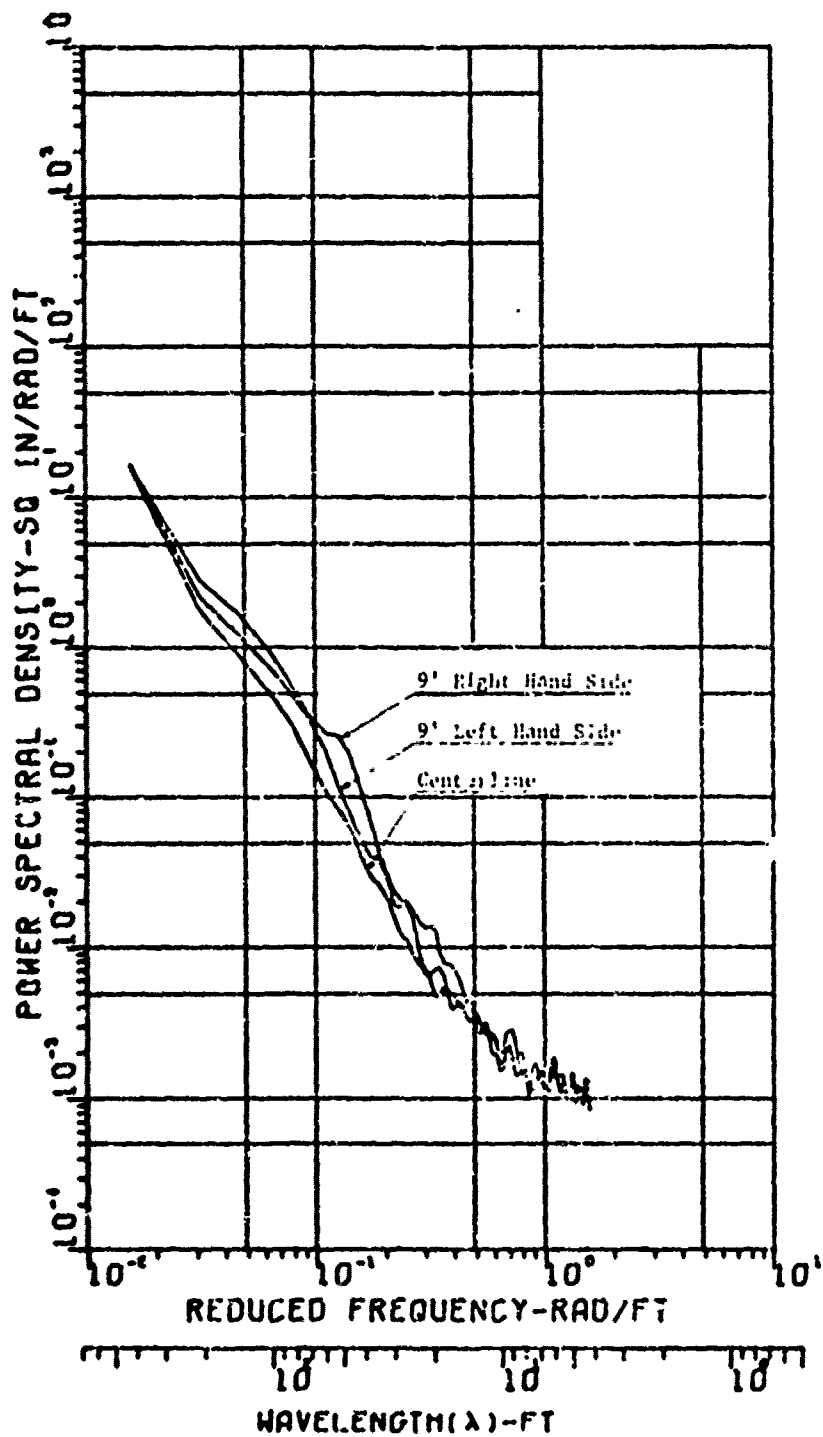


Figure 7. PSD of Washington National Airport Runway 36

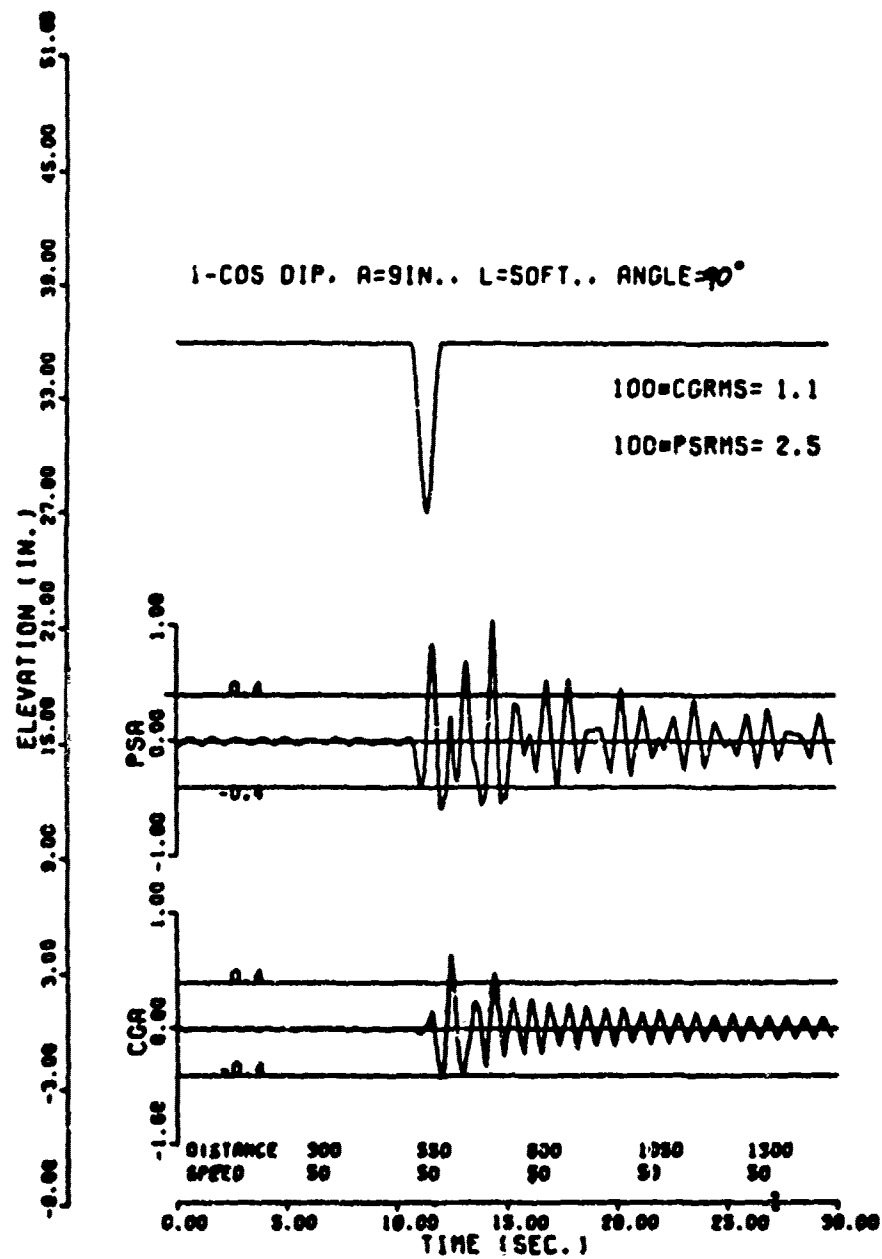


Figure 8. Boeing 727-100 Traversing a (1-cos) dip head-on.

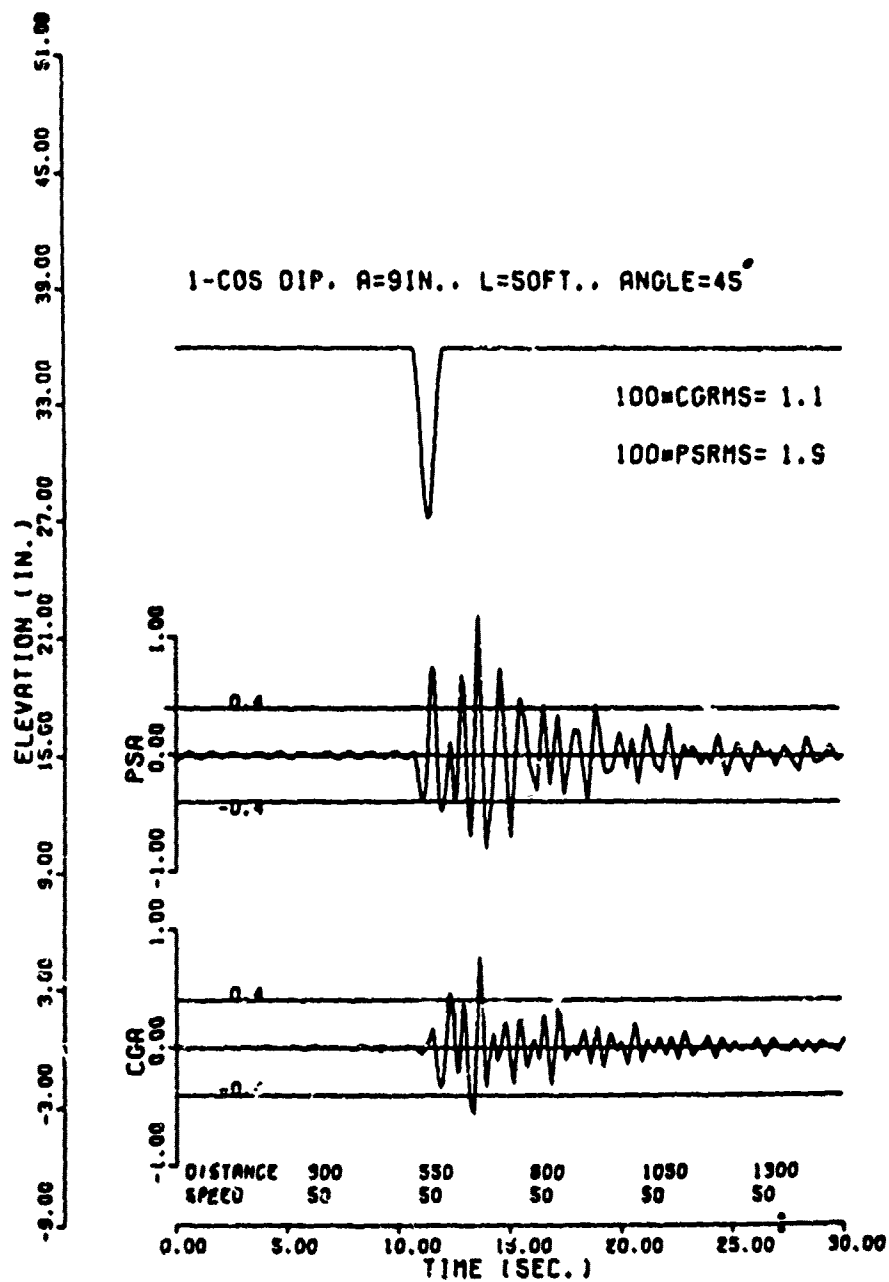


Figure 9. Boeing 727-100 Traversing a (1-cos) dip at a 45° angle

Figures 10 and 11 show the plotted results of the C-9A and AMST respectively hitting the 1-cos dip at a 45° angle at a constant speed of 50 fps. While the C-9A had a relatively high response, the AMST, which is designed to operate off of rough fields, "absorbed" the dip to a large degree. This indicates that the computer program is calculating relative responses which are at least intuitively correct.

Up to this point only constant speed simulations have been discussed. Figures 12, 13 and 14 show the plotted results of the Boeing 727-100, AMST and the C-9A respectively taking off from the Washington National runway profile. Takeoff simulations are made by starting at a near zero forward velocity and accelerating at a constant thrust until rotation speed is reached, then the simulation is terminated. Again it can be seen that the AMST (which is designed for rough field operation) had a very low dynamic response, even though this runway is relatively rough. Figure 15 shows the plotted PSD's of Washington National Runway 36 and of two typically smooth runways, one at Portland Oregon and one at Dulles International. The Washington National Runway is significantly rougher.

Experimental data was available for comparison with the 727-100 takeoff simulation. Figure 16 shows the actual time history plots of vertical acceleration measured on a 727-100 taking off at 120,000 pounds gross weight from Washington National Runway 36 on December 11, 1972. Some parameters of the test aircraft were unknown such as strut and tire pressures and actual inertias. So exact simulation was not possible. However, Table 4 shows that comparison of several peak values of vertical accelerations at the P.S. were within 15 percent. The comparisons of C.G. vertical accelerations were not as good. In the simulation the acceleration levels were lower. It appears that main gear strut pressures on the actual airplane were lower than that simulated. This difference would cause the higher response in the plunge mode.

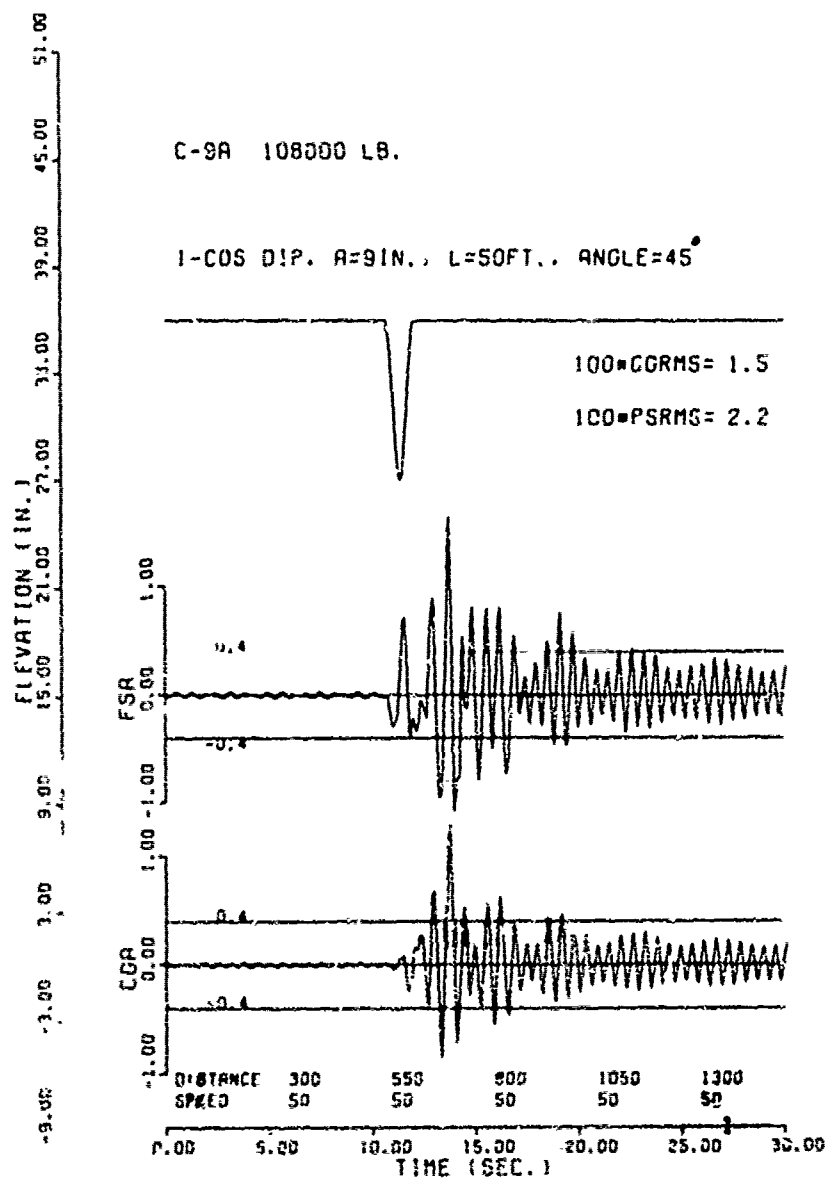


Figure 10. C-9A Traversing a (1-cos) dip at a 45° angle

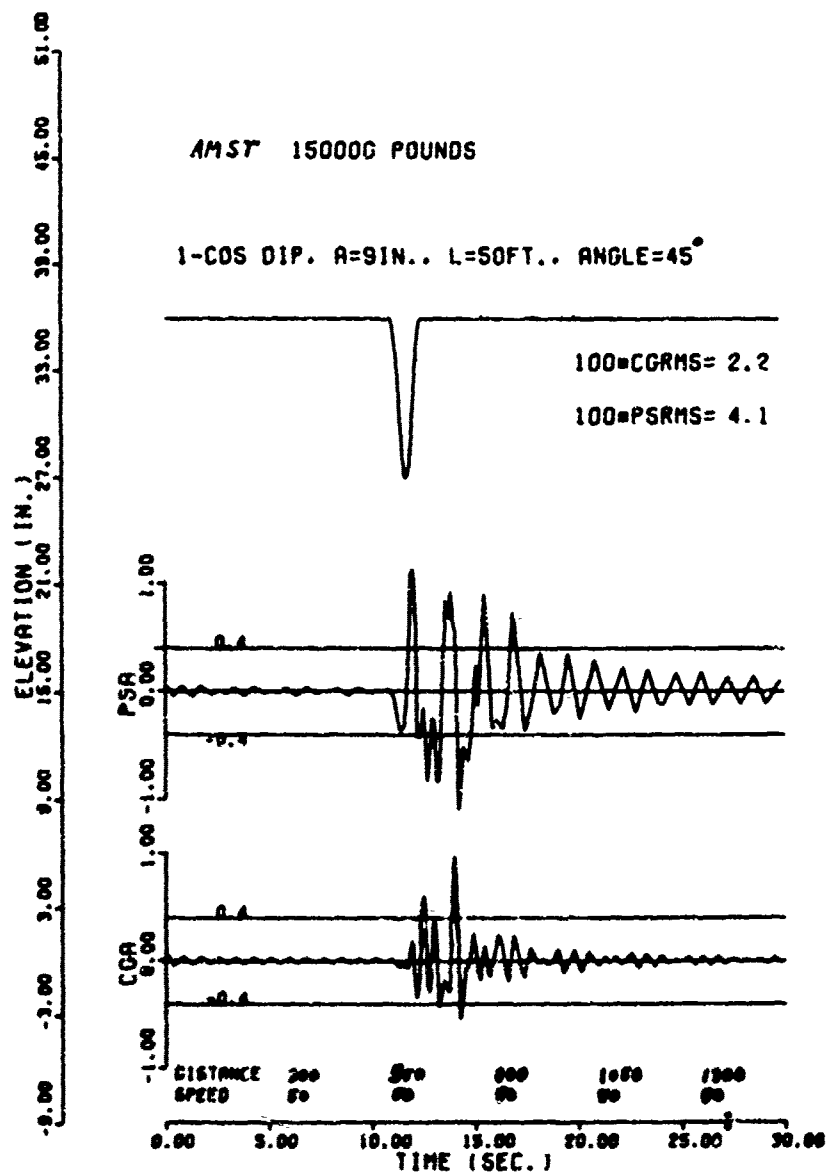


Figure 11. AMST Traversing a (1-cos) dip at a 45° angle

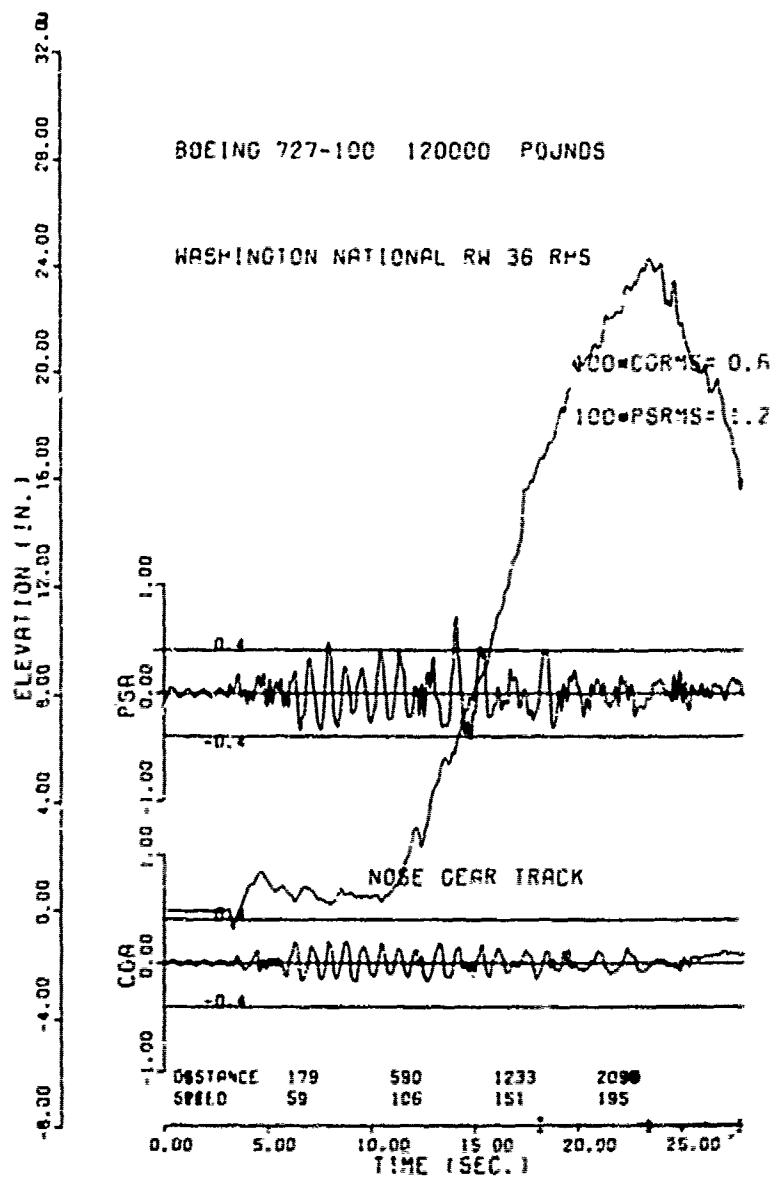


Figure 12. Boeing 727-100 Taking Off from Washington National Airport With the Roll Degree of Freedom Included

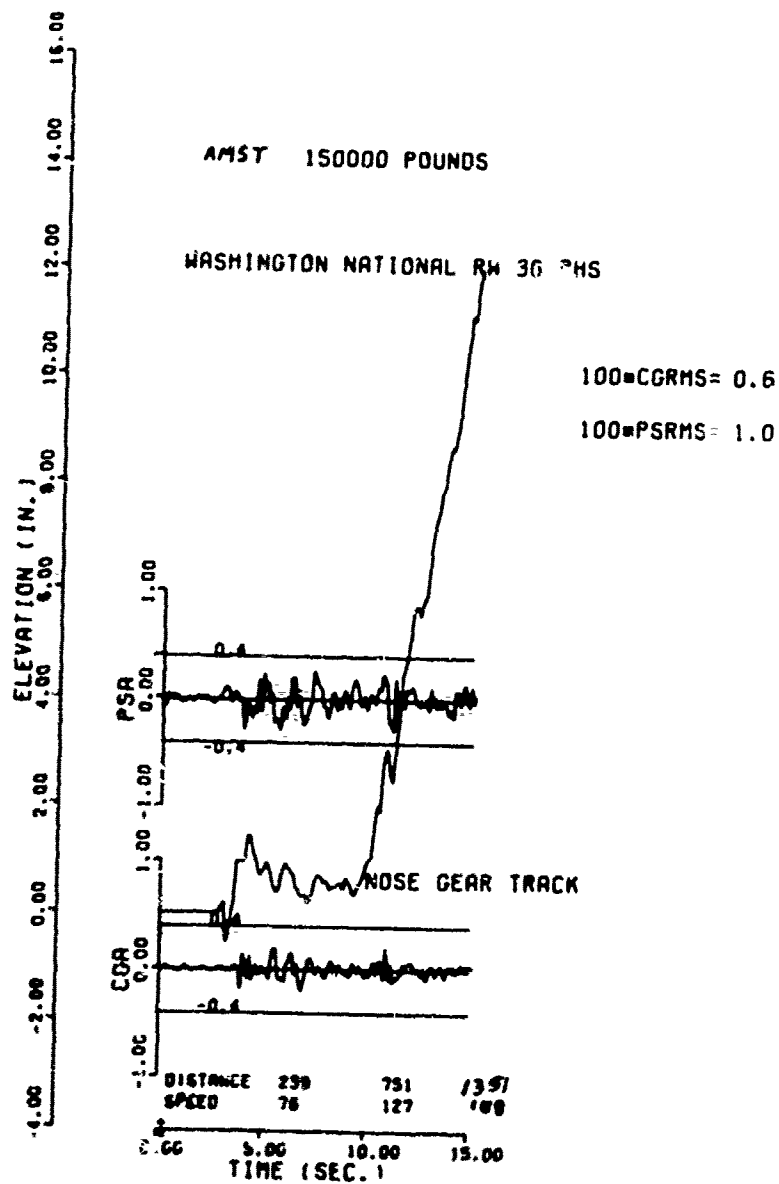


Figure 13. AMST Taking Off from Washington National Airport With the Roll Degree of Freedom Included

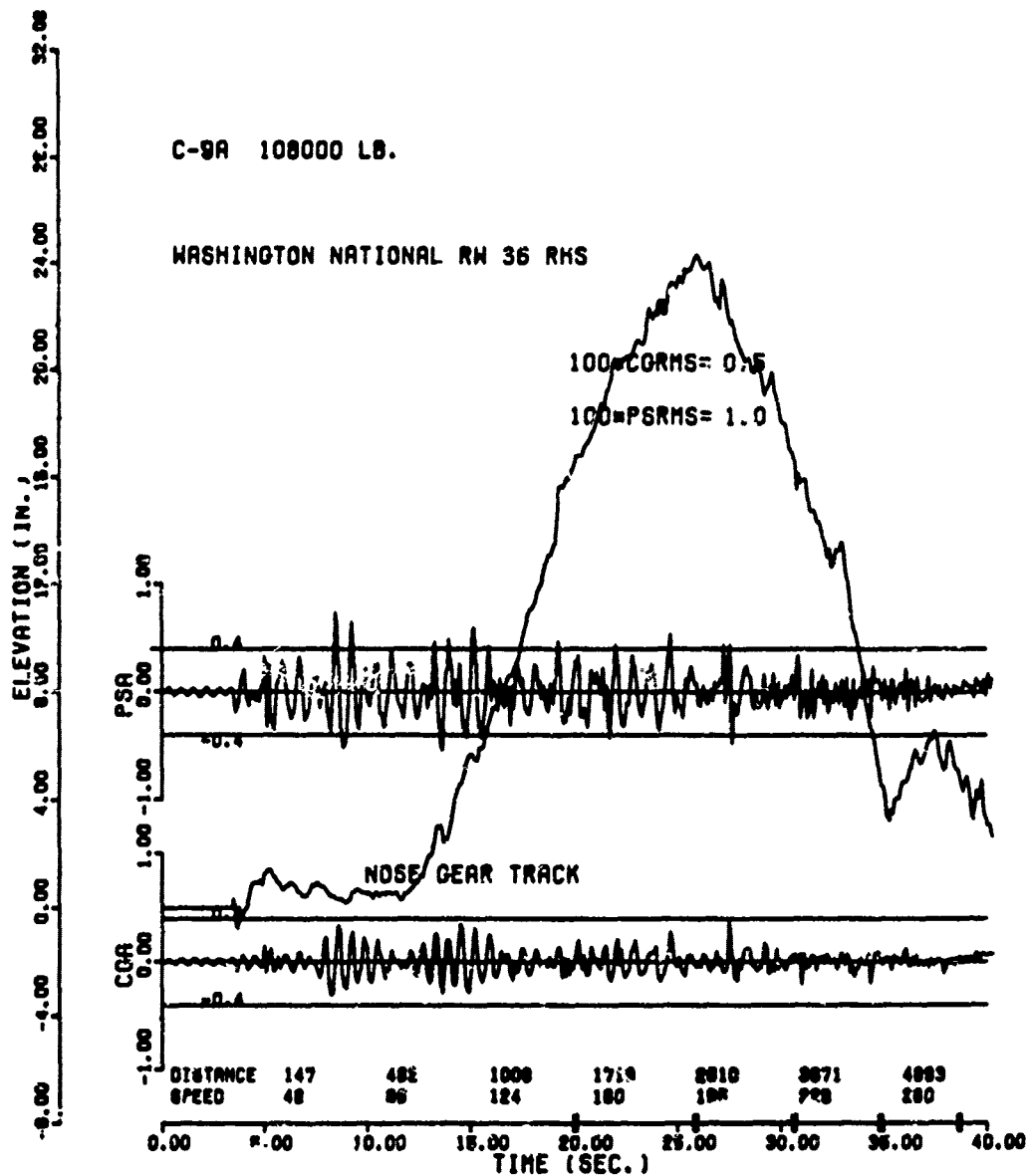


Figure 14. C-9A Taking Off from Washington National Airport With the Roll Degree of Freedom Included

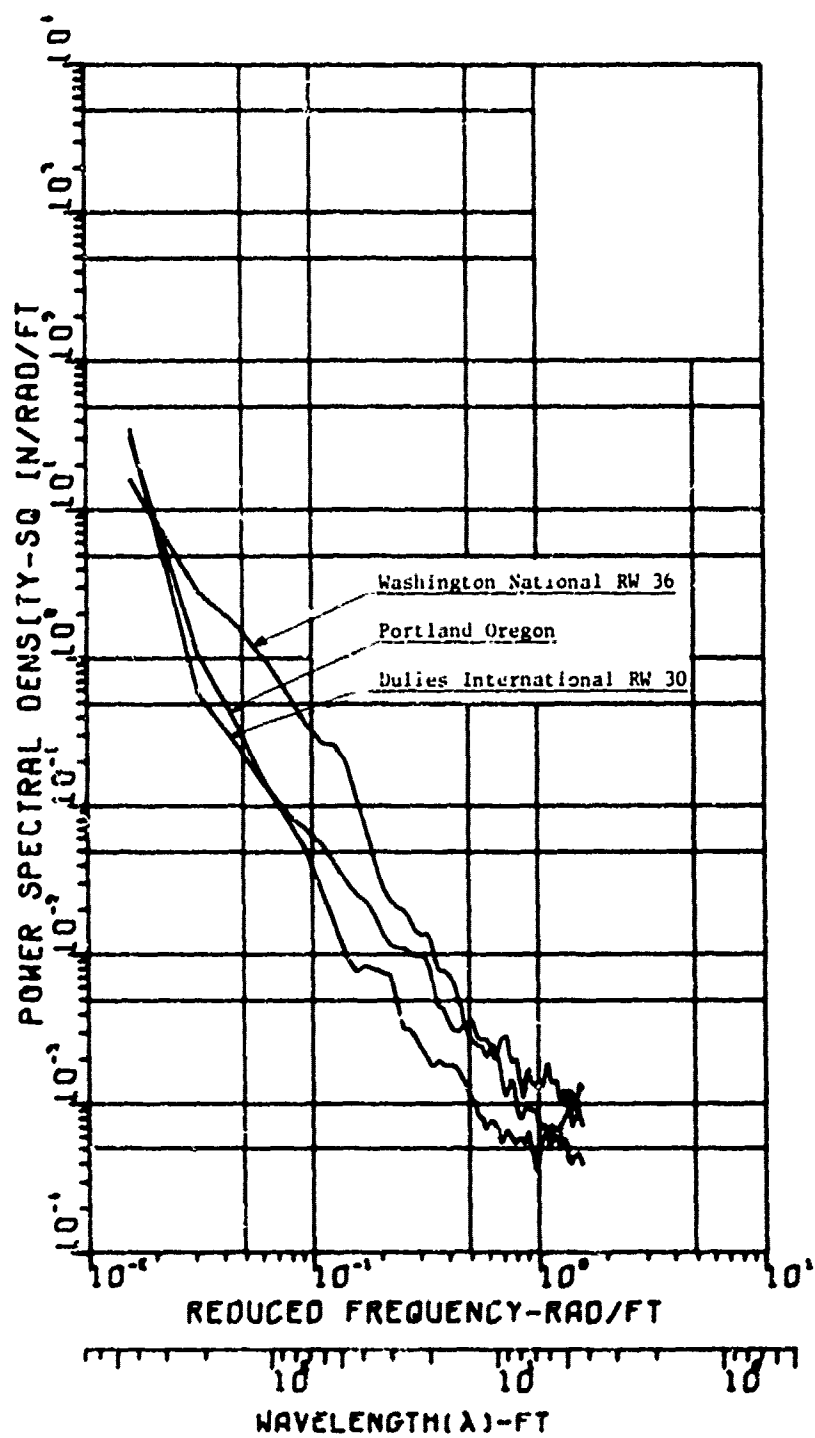


Figure 15. PSD of Washington National Runway 36 and two Typically Smooth Runways

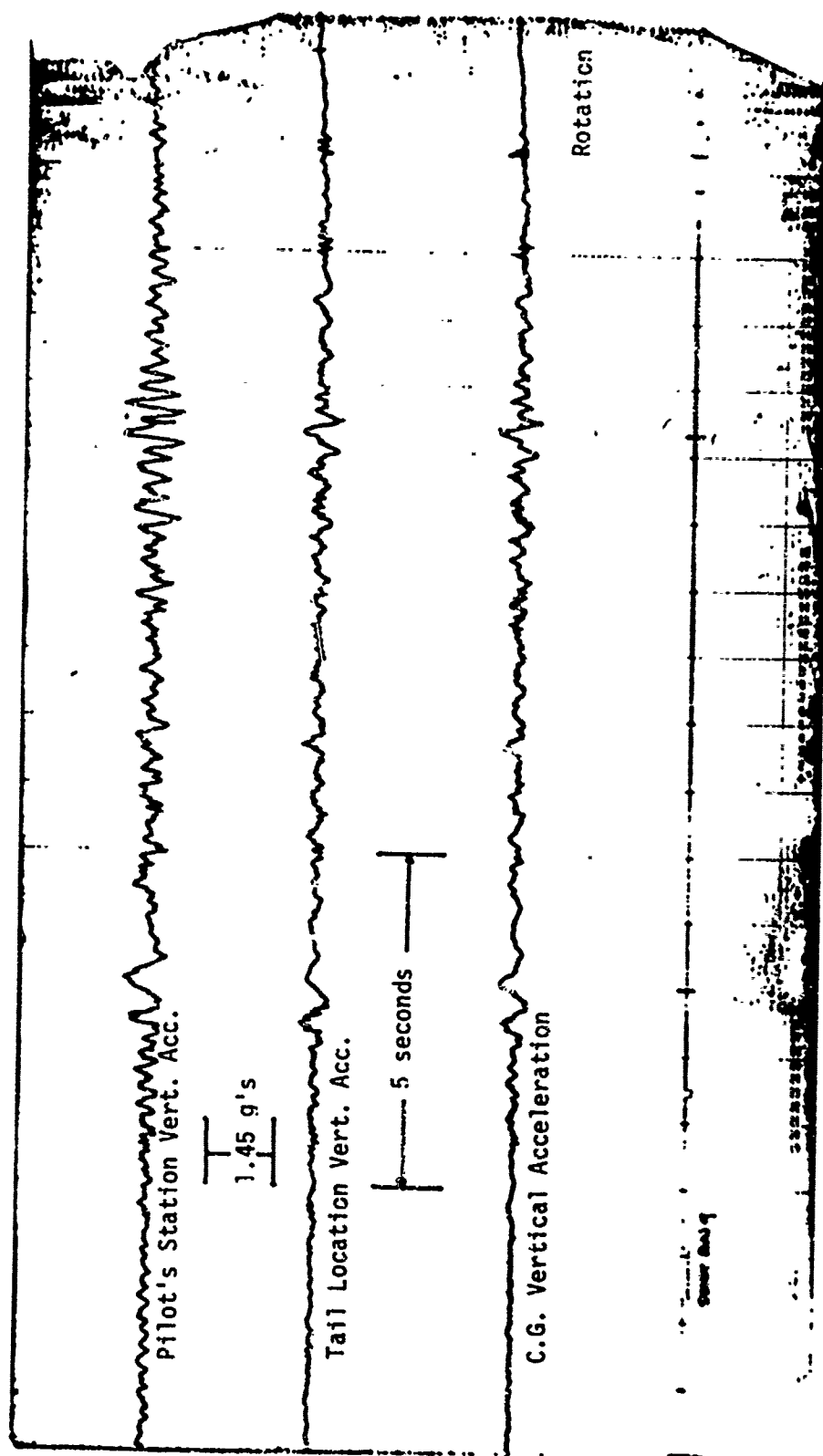


Figure 16. Measured Response of a Boeing 727-100 Takeoff at Washington National Airport Runway 36

TABLE 4
COMPARISONS OF SIMULATED AND EXPERIMENTAL DATA

Experimental Time (sec)	<u>P.S. Vertical Acceleration</u>		<u>C.G. Vertical Acceleration</u>	
	Exp (g's)	Sim (g's)	Exp (g's)	Sim (g's)
8.0	0.9425	0.90	0.55	0.35
16.3	1.305	1.12	0.80	0.40
20.5	TAKEOFF			

Note: All measurements are measured from peak to peak.

The remaining simulations made were with the inclusion of wing flexibility in the simulations. The purpose of including the wing flexibility was to see if there was a significant change in P.S. and C.G. vertical acceleration response when the wing was permitted to bend when acted on by a main landing gear strut force. These simulations were made on the C-9A only because this was the only aircraft for which wing flexibility data was available. Figure 17 shows the plotted results of C-9A with flexible wings traversing the 1-cos dip at a 45° angle. This figure can be compared to Figure 10 which is the same simulation without flexible wings. By superimposing the two plots it was determined after T=17 seconds, small changes in vertical acceleration were appearing in both the P.S. and C.G. responses. Generally the higher accelerations occurred on the C-9A simulation with flexible wings. Also there was a phase lag. By the end of the run the rigid wing model lagged the flexible wing model by approximately one half of a cycle. Figure 18 shows the plotted response of the C-9A with flexible wings during a takeoff simulation from Washington National Runway 36. Figure 14 shows the same simulation without flexible wings. Superposition of the two plots shows little change, if any, in the airplane's response.

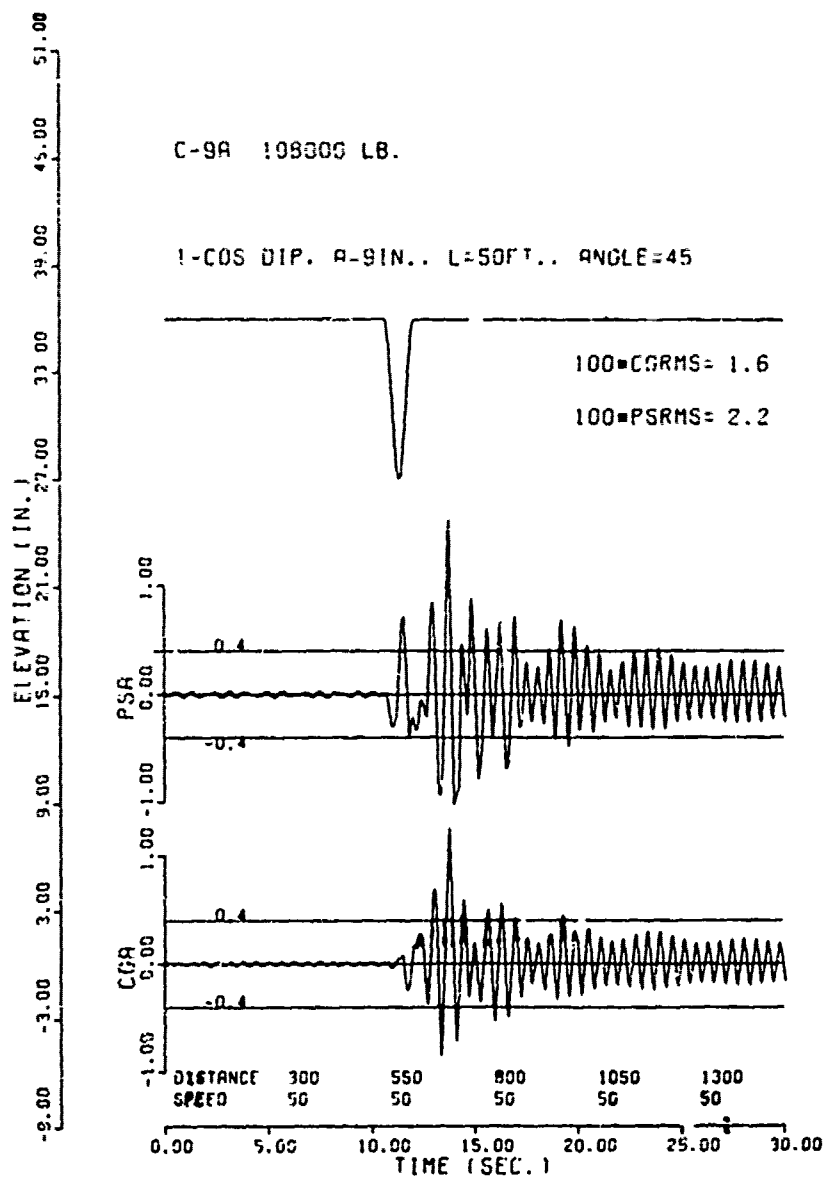


Figure 17. C-9A with Flexible Wings Taxiing over a (1-cos) dip at a 45° angle

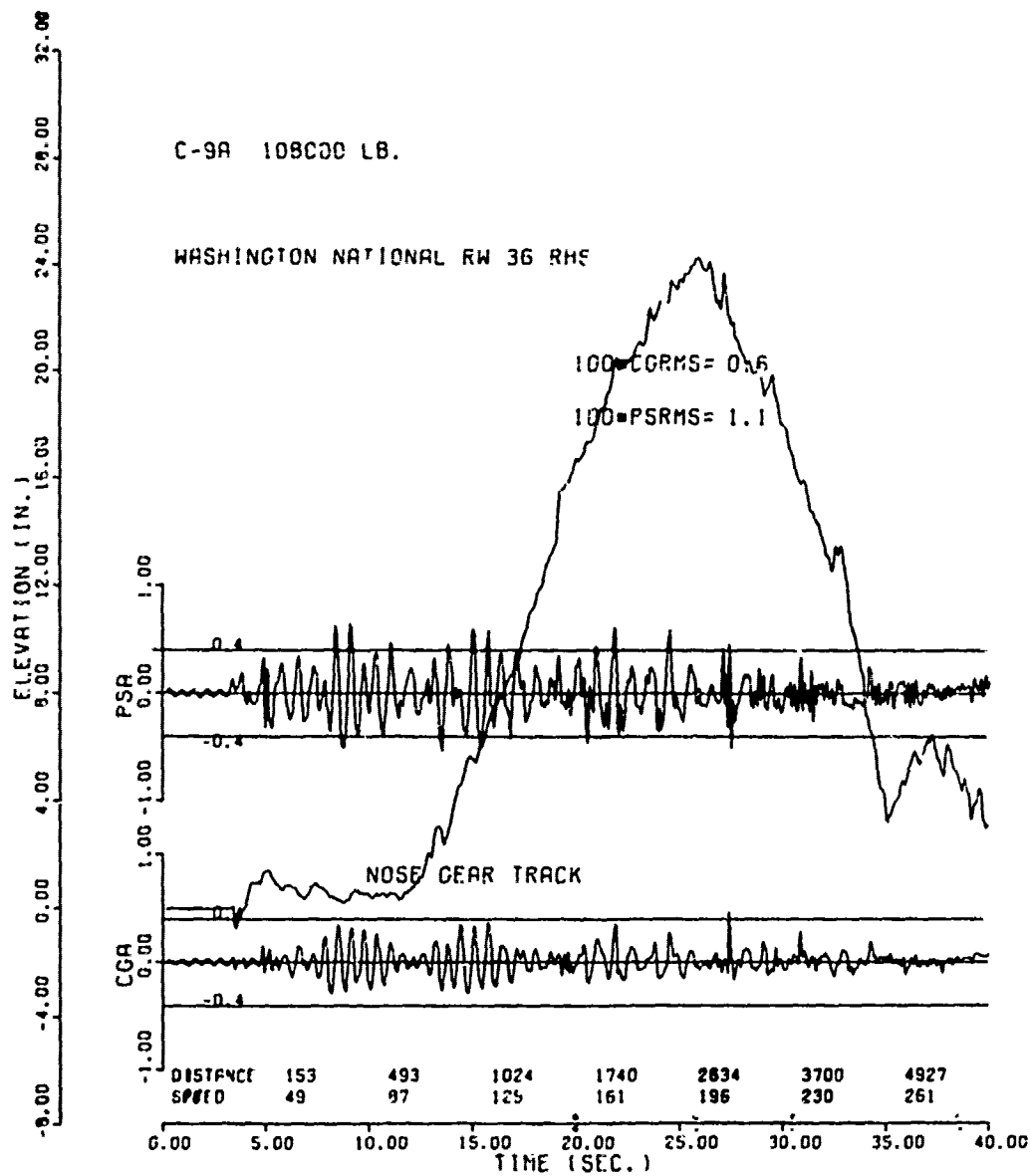


Figure 18. C-9A with Flexible Wings Taking Off from Washington National Runway 36

SECTION V

SUMMARY AND CONCLUSIONS

In summary, a mathematical model has been formulated and programmed for a digital computer and is capable of simulating most flexible aircraft traversing an unsymmetric runway profile during constant speed taxi or takeoff. Three different aircraft have been simulated and comparisons have been made with experimental data.

Based on the 11 simulations made, the following conclusions were drawn:

1. The roll degree of freedom has a significant effect on the pilot's station and center of gravity vertical acceleration levels if the runway profile is asymmetric. The degree is dependent upon how asymmetric the profile is.
2. The effect of wing flexibility on F.S. and C.G. vertical acceleration response is small enough to be neglected, at least for the airplane simulated (C-9A). However, with the addition of flexible wings, it now becomes an easy matter to expand the computer program to obtain vertical accelerations (and consequently shears and moments) at vital wing stations such as the wing root and engine and stores pylons. This would be a natural extension of the study.
3. Comparison of the simulated aircraft response with the limited amount of available test data was satisfactory. The roughest parts of the runway were identified and, as in the test, pilot station acceleration levels exceeded the $\pm 0.4g$ criterion. If exact strut and tire pressures, and inertia's were known for the test aircraft, the simulated C.G. response may have more closely matched the experimental data.

The simulated takeoff took an additional 5 seconds to reach rotation speed. It is assumed that the actual test aircraft weight was less than 120,000 pounds, because several runs were made without refueling the aircraft after each run. Therefore, some of the fuel had been burned off. The fact that the airplane was lighter than

that simulated would also contribute to the difference in C.G. response. Also, using a 15° flap setting changed the value of C_L and resulted in a shorter takeoff distance.

4. This computer program, "TAX2", appears to be a very efficient technique for locating the rough areas of an asymmetric runway. Using a CDC 6600 digital computer, a C-9A takeoff simulation required 70 seconds of central processor (CP) computer time, which is just 30 seconds over real time for this simulation. These numbers are typical for most simulations.

One of the advantages of a program of this type is that runway repairs can be simulated before the actual repair is made in order to determine the minimum amount of repair required. In addition, the effect of the proposed repair on other aircraft can be determined before the repair is made.

AFFDL-TR-77-37

APPENDIX A
DEVELOPMENT OF EQUATIONS OF MOTION

Development of equations of motion using Lagrange equations. All symbols refer to Figure A-1.

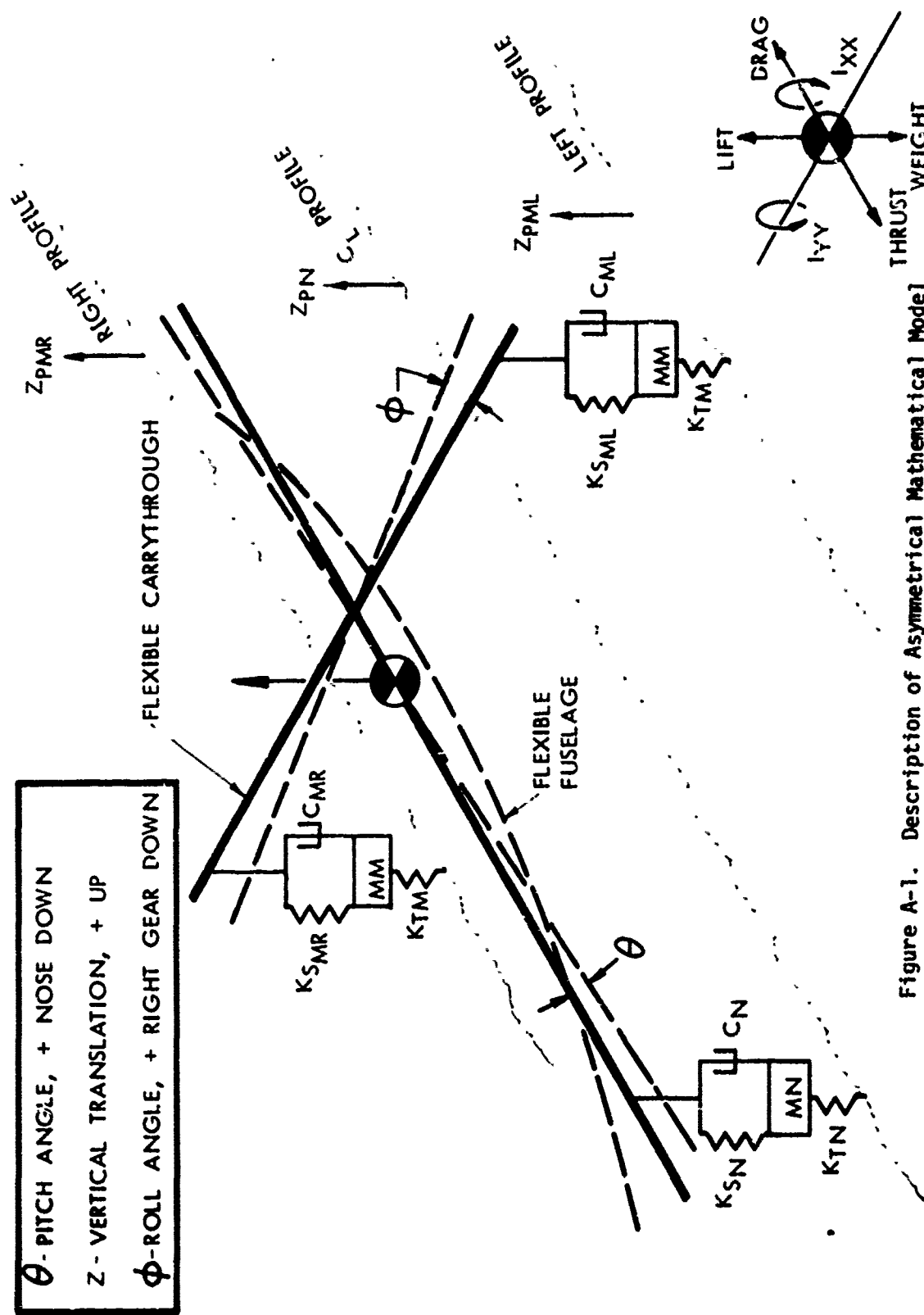


Figure A-1. Description of Asymmetrical Mathematical Model

Using Lagrange

$$\frac{d}{dt} \frac{\partial KE}{\partial \dot{q}_i} - \frac{\partial KE}{\partial q_i} + \frac{\partial PE}{\partial q_i} + \frac{\partial DE}{\partial \dot{q}_i} = 0$$

The Kinetic Energy is:

$$K.E. = \frac{1}{2} \dot{Z}_{cg}^2 + \frac{1}{2} M \dot{Z}_{MR}^2 + \frac{1}{2} M \dot{Z}_{ML}^2 \\ + \frac{1}{2} M \dot{Z}_N^2 + \frac{1}{2} I_{yy} \dot{\theta}^2 + \frac{1}{2} I_{xx} \dot{\phi}^2$$

The Potential Energy is:

$$P.E. = + W_M Z_{MR} + W_M Z_{ML} + W_N Z_N + W Z_{cg} - L Z_{cg} \\ + \frac{1}{2} K_{SML} (Z_{cg} + A\theta - Z_{ML} - C\phi)^2 + \frac{1}{2} K_{TML} (Z_{ML} - Z_{PML})^2 \\ + \frac{1}{2} K_{SMR} (Z_{cg} + A\theta - Z_{MR} + C\phi)^2 + \frac{1}{2} K_{TMR} (Z_{MR} - Z_{PMR})^2 \\ + \frac{1}{2} K_{SN} (Z_{cg} - B\theta - Z_N)^2 + \frac{1}{2} K_{TN} (Z_N - Z_{PN})^2$$

The Dissipative Energy is:

$$D.E. = + \frac{1}{2} C_{ML} (\dot{Z}_{cg} + A\dot{\theta} - \dot{Z}_{ML} - C\dot{\phi})^2 \\ + \frac{1}{2} C_{MR} (\dot{Z}_{cg} + A\dot{\theta} - \dot{Z}_{MR} + C\dot{\phi})^2 \\ + \frac{1}{2} C_N (\dot{Z}_{cg} - B\dot{\theta} - \dot{Z}_N)^2$$

Now Find $\frac{d}{dt} \frac{\partial KE}{\partial \dot{q}_i}$

$$\frac{d}{dt} \frac{\partial KE}{\partial \dot{Z}_{cg}} = M \ddot{Z}_{cg} ; \frac{d}{dt} \frac{\partial KE}{\partial \dot{Z}_N} = M \ddot{Z}_N$$

$$\frac{d}{dt} \frac{\partial KE}{\partial \dot{Z}_{MR}} = M \ddot{Z}_{MR} ; \frac{d}{dt} \frac{\partial KE}{\partial \dot{\theta}} = I_{yy} \ddot{\theta}$$

$$\frac{d}{dt} \frac{\partial KE}{\partial \dot{Z}_{ML}} = M \ddot{Z}_{ML} ; \frac{d}{dt} \frac{\partial KE}{\partial \dot{\phi}} = I_{xx} \ddot{\phi}$$

$$\frac{\partial KE}{\partial q_i} = 0$$

Now Find $\frac{\partial(P.E)}{\partial q_i}$

$$\frac{\partial(P.E)}{\partial Z_{cg}} = + K_{SML}(Z_{cg} + A\theta - Z_{ML} - C\phi)$$

$$+ K_{SMR}(Z_{cg} + A\theta - Z_{MR} + C\phi)$$

$$+ K_{SN}(Z_{cg} - B\theta - Z_N) + W - L$$

$$\frac{\partial(P.E)}{\partial Z_{MR}} = + W_M - K_{SMR}(Z_{cg} + A\theta - Z_{MR} + C\phi)$$

$$+ K_{TM}(Z_{MR} - Z_{PMR})$$

$$\frac{\partial(P.E)}{\partial Z_{ML}} = + W_M - K_{SML}(Z_{cg} + A\theta - Z_{ML} - C\phi)$$

$$+ K_{TM}(Z_{ML} - Z_{PML})$$

$$\frac{\partial(P.E)}{\partial Z_N} = + W_N - K_{SN}(Z_{cg} - B\theta - Z_N) + K_{TN}(Z_N - Z_{PN})$$

$$\frac{\partial(P.E)}{\partial \theta} = + K_{SML}A(Z_{cg} + A\theta - Z_{ML} - C\phi)$$

$$+ K_{SMR}A(Z_{cg} + A\theta - Z_{MR} + C\phi)$$

$$- K_{SN}B(Z_{cg} - B\theta - Z_N)$$

$$\frac{\partial(P.E)}{\partial \phi} = - K_{SML}C(Z_{cg} + A\theta - Z_{ML} - C\phi)$$

$$+ K_{SMR}C(Z_{cg} + A\theta - Z_{MR} + C\phi)$$

Now Find $\frac{\partial(D.E)}{\partial \dot{q}_i}$

$$\frac{\partial(D.E)}{\partial \dot{Z}_{MR}} = - C_{MR}(\dot{Z}_{cg} + A\dot{\theta} - \dot{Z}_{MR} + C\dot{\phi})$$

$$\frac{\partial (D.E)}{\partial \dot{Z}_{ML}} = - C_{ML} (\dot{Z}_{cg} + A\dot{\theta} - \dot{Z}_{ML} - C\dot{\phi})$$

$$\frac{\partial (D.E)}{\partial \dot{Z}_N} = - C_N (\dot{Z}_{cg} - B\dot{\theta} - \dot{Z}_N)$$

$$\begin{aligned} \frac{\partial (D.E)}{\partial \dot{Z}_{cg}} &= + C_{MR} (\dot{Z}_{cg} + A\dot{\theta} - \dot{Z}_{MR} + C\dot{\phi}) \\ &\quad + C_{ML} (\dot{Z}_{cg} + A\dot{\theta} - \dot{Z}_{ML} - C\dot{\phi}) \\ &\quad - C_N (\dot{Z}_{cg} - B\dot{\theta} - \dot{Z}_N) \end{aligned}$$

$$\begin{aligned} \frac{\partial (D.E)}{\partial \dot{\theta}} &= + C_{MR} A (\dot{Z}_{cg} + A\dot{\theta} - \dot{Z}_{MR} + C\dot{\phi}) \\ &\quad + C_{ML} A (\dot{Z}_{cg} + A\dot{\theta} - \dot{Z}_{ML} - C\dot{\phi}) \\ &\quad - C_N B (\dot{Z}_{cg} - B\dot{\theta} - \dot{Z}_N) \end{aligned}$$

$$\begin{aligned} \frac{\partial (D.E)}{\partial \dot{\phi}} &= + C_{MR} C (\dot{Z}_{cg} + A\dot{\theta} - \dot{Z}_{MR} + C\dot{\phi}) \\ &\quad - C_{ML} C (\dot{Z}_{cg} + A\dot{\theta} - \dot{Z}_{ML} - C\dot{\phi}) \end{aligned}$$

Combine Terms

$$\begin{aligned} M\ddot{Z}_{cg} &= - K_{SML} [Z_{cg} + A\dot{\theta} - \dot{Z}_{ML} - C\dot{\phi}] \\ &\quad - K_{SMR} [Z_{cg} + A\dot{\theta} - \dot{Z}_{MR} + C\dot{\phi}] \\ &\quad - K_{SN} [Z_{cg} - B\dot{\theta} - \dot{Z}_N] - W + L \\ &\quad - C_{MR} [\dot{Z}_{cg} + A\dot{\theta} - \dot{Z}_{MR} + C\dot{\phi}] \\ &\quad - C_{ML} [\dot{Z}_{cg} + A\dot{\theta} - \dot{Z}_{ML} - C\dot{\phi}] \\ &\quad - C_N [\dot{Z}_{cg} - B\dot{\theta} - \dot{Z}_N] \end{aligned}$$

Rewriting we have

$$M\ddot{Z}_{cg} = [-K_{SML}(x_{ML}) - C_{ML}(\dot{x}_{ML})] + \quad (1)$$

$$[-K_{SMR}(x_{MR}) - C_{MR}(\dot{x}_{MR})] +$$

$$[-K_{SN}(x_N) - C_N(\dot{x}_N)] - W + L$$

where the terms in the brackets are the left, right, and nose landing gear strut forces respectively.

Similarly

$$M \ddot{z}_{ML} = K_{SML}(x_{ML}) + C_{ML}(\dot{x}_{ML}) \quad (2)$$

$$- K_{TM}(z_{ML} - z_{PML}) - W_M$$

$$M \ddot{z}_{MR} = K_{SMR}(x_{MR}) + C_{MR}(\dot{x}_{MR}) \quad (3)$$

$$- K_{TM}(z_{MR} - z_{PMR}) - W_M$$

$$M \ddot{z}_N = K_{SN}(x_N) + C_N(\dot{x}_N) - K_{TN}(z_N - z_{PN}) \quad (4)$$

$$I_{yy} \ddot{\theta} = -K_{SML}A(x_{ML}) + C_{ML}A(\dot{x}_{ML})$$

$$+ K_{SMR}A(x_{MR}) + C_{MR}A(\dot{x}_{MR}) \quad (5)$$

$$- K_N B(x_N) + C_N B(\dot{x}_N)$$

$$I_{xy} \ddot{\phi} = K_{SML}C(x_{ML}) + C_{ML}C(\dot{x}_{ML}) \quad (6)$$

$$- K_{SMR}C(x_{MR}) - C_{MR}C(\dot{x}_{MR})$$

The Forward Translation Equation of Motion is uncoupled and expressed as follows:

$$M\ddot{X} = T - D_a - D_t$$

where:

T = Thrust

D_a = Aerodynamic Drag

D_t = Tire Drag (Total)

The modal method will be used to express the aircraft's flexibility as follows:

$$M_i \ddot{q}_i = \xi_{ij} F_j - 2\zeta \omega_i M_i \dot{q}_i - \omega_i^2 M_i q_i$$

where i = the i th mode

F_j = the j th force input into the system (such as strut force)

M_i = the i th generalized mass

q_i = the generalized coordinate

ξ_{ij} = the modal deflection of the i th mode at fuselage station j for symmetric modes or wing station j for asymmetric modes.

ω_i = the i th mode natural frequency

ζ = Structural damping factor

By using this technique the displacements X'_{MR} , X'_{ML} , X'_N and their time derivatives reflect the motion of the bending fuselage and wings by adding the $\sum_{i=1}^N q_i \xi_{ij}$ (modal displacements) at the j th (required location).

For example;

$$\text{Total Displacement } X'_{MR} = X_{MR} + \sum_{i=1}^N q_i \xi_{iR} + \sum_{k=1}^P q_k \xi_{kR}$$

$$\text{Total Velocity } \dot{X}'_{MR} = \dot{X}_{MR} + \sum_{i=1}^N \dot{q}_i \xi_{iR} + \sum_{k=1}^P \dot{q}_k \xi_{kR}$$

where:

Term 1 = Displacements of the rigid body

Term 2 = Displacements due to the symmetric modes

Term 3 = Displacements due to the asymmetric modes

AFFDL-TR-77-37

APPENDIX B
LISTING OF COMPUTER PROGRAM TAX2

49

04000-4 1A12 76/76 72121

[illegible]

PROGRAM TAX2 75/76 OPT=1

[illegible]

15129175 10.22.20

FTN 6.549436

7A131

RECEIVED 2147

[illegible]

2

1.

[illegible]

1000

PROGRAM T-112

[illegible]

BEST AVAILABLE COPY

PROGRAM	TAKE	70/74	001-1	FTM 0.50000	18.22.04	DATE	T
345	105	MM = MM + 1 GOTO(100) = STORE2 PROFIMA = 100 TIME(100) = 100 IF TIME(100) > 100 THEN TIME(100) = .01 STORE1 = STORE2 STORE2 = STORE1 100 IF (ABS(PSA) < ABS(STORE1) AND ABS(STORE1) < ABS(STORE2)) 200 STORE3 = STORE1 GO TO 210 205 IF (X-TIME(100) < 0) GO TO 210 IF (ABS(STORE1) < ABS(STORE2)) GO TO 210 210 LL = LL + 1 PRAC(100) = STORE1 TIME(100) = 100 IF TIME(100) < 100 THEN TIME(100) = .01 STORE1 = STORE2 STORE2 = STORE1 215 IF (ABS(100) < ABS(100) < 5.0) GO TO 220 220 IF (100 < 100) GO TO 225 PRAC(100) = 100 MM = MM + 1000 IF (100 < 100) GO TO 230 225 IF (ABS(100) < 5.0) GO TO 230 230 IF (100 < 100) GO TO 235 235 IF (100 < 100) GO TO 235 240 IF (100 < 100) GO TO 240 CALL TAYLOR(10, 100) IF (100 < 100) GO TO 240 IF (100 < 100) GO TO 240 TIME = TIME + 0.1 GOTO 100 245 IF (100 < 100) GO TO 245 250 IF (100 < 100) GO TO 250 255 IF (100 < 100) GO TO 255 260 IF (100 < 100) GO TO 260 265 IF (100 < 100) GO TO 265 270 IF (100 < 100) GO TO 270 275 IF (100 < 100) GO TO 275 280 IF (100 < 100) GO TO 280 285 IF (100 < 100) GO TO 285 290 IF (100 < 100) GO TO 290 295 IF (100 < 100) GO TO 295 300 IF (100 < 100) GO TO 300 305 IF (100 < 100) GO TO 305 310 IF (100 < 100) GO TO 310 315 IF (100 < 100) GO TO 315 320 IF (100 < 100) GO TO 320 325 IF (100 < 100) GO TO 325 330 IF (100 < 100) GO TO 330 335 IF (100 < 100) GO TO 335 340 IF (100 < 100) GO TO 340 345 IF (100 < 100) GO TO 345 350 IF (100 < 100) GO TO 350 355 IF (100 < 100) GO TO 355 360 IF (100 < 100) GO TO 360 365 IF (100 < 100) GO TO 365 370 IF (100 < 100) GO TO 370 375 IF (100 < 100) GO TO 375 380 IF (100 < 100) GO TO 380 385 IF (100 < 100) GO TO 385 390 IF (100 < 100) GO TO 390 395 IF (100 < 100) GO TO 395 400 IF (100 < 100) GO TO 400 405 IF (100 < 100) GO TO 405 410 IF (100 < 100) GO TO 410 415 IF (100 < 100) GO TO 415 420 IF (100 < 100) GO TO 420 425 IF (100 < 100) GO TO 425 430 IF (100 < 100) GO TO 430 435 IF (100 < 100) GO TO 435 440 IF (100 < 100) GO TO 440 445 IF (100 < 100) GO TO 445 450 IF (100 < 100) GO TO 450 455 IF (100 < 100) GO TO 455 460 IF (100 < 100) GO TO 460 465 IF (100 < 100) GO TO 465 470 IF (100 < 100) GO TO 470 475 IF (100 < 100) GO TO 475 480 IF (100 < 100) GO TO 480 485 IF (100 < 100) GO TO 485 490 IF (100 < 100) GO TO 490 495 IF (100 < 100) GO TO 495 500 IF (100 < 100) GO TO 500 505 IF (100 < 100) GO TO 505 510 IF (100 < 100) GO TO 510 515 IF (100 < 100) GO TO 515 520 IF (100 < 100) GO TO 520 525 IF (100 < 100) GO TO 525 530 IF (100 < 100) GO TO 530 535 IF (100 < 100) GO TO 535 540 IF (100 < 100) GO TO 540 545 IF (100 < 100) GO TO 545 550 IF (100 < 100) GO TO 550 555 IF (100 < 100) GO TO 555 560 IF (100 < 100) GO TO 560 565 IF (100 < 100) GO TO 565 570 IF (100 < 100) GO TO 570 575 IF (100 < 100) GO TO 575 580 IF (100 < 100) GO TO 580 585 IF (100 < 100) GO TO 585 590 IF (100 < 100) GO TO 590 595 IF (100 < 100) GO TO 595 600 IF (100 < 100) GO TO 600 605 IF (100 < 100) GO TO 605 610 IF (100 < 100) GO TO 610 615 IF (100 < 100) GO TO 615 620 IF (100 < 100) GO TO 620 625 IF (100 < 100) GO TO 625 630 IF (100 < 100) GO TO 630 635 IF (100 < 100) GO TO 635 640 IF (100 < 100) GO TO 640 645 IF (100 < 100) GO TO 645 650 IF (100 < 100) GO TO 650 655 IF (100 < 100) GO TO 655 660 IF (100 < 100) GO TO 660 665 IF (100 < 100) GO TO 665 670 IF (100 < 100) GO TO 670 675 IF (100 < 100) GO TO 675 680 IF (100 < 100) GO TO 680 685 IF (100 < 100) GO TO 685 690 IF (100 < 100) GO TO 690 695 IF (100 < 100) GO TO 695 700 IF (100 < 100) GO TO 700 705 IF (100 < 100) GO TO 705 710 IF (100 < 100) GO TO 710 715 IF (100 < 100) GO TO 715 720 IF (100 < 100) GO TO 720 725 IF (100 < 100) GO TO 725 730 IF (100 < 100) GO TO 730 735 IF (100 < 100) GO TO 735 740 IF (100 < 100) GO TO 740 745 IF (100 < 100) GO TO 745 750 IF (100 < 100) GO TO 750 755 IF (100 < 100) GO TO 755 760 IF (100 < 100) GO TO 760 765 IF (100 < 100) GO TO 765 770 IF (100 < 100) GO TO 770 775 IF (100 < 100) GO TO 775 780 IF (100 < 100) GO TO 780 785 IF (100 < 100) GO TO 785 790 IF (100 < 100) GO TO 790 795 IF (100 < 100) GO TO 795 800 IF (100 < 100) GO TO 800 805 IF (100 < 100) GO TO 805 810 IF (100 < 100) GO TO 810 815 IF (100 < 100) GO TO 815 820 IF (100 < 100) GO TO 820 825 IF (100 < 100) GO TO 825 830 IF (100 < 100) GO TO 830 835 IF (100 < 100) GO TO 835 840 IF (100 < 100) GO TO 840 845 IF (100 < 100) GO TO 845 850 IF (100 < 100) GO TO 850 855 IF (100 < 100) GO TO 855 860 IF (100 < 100) GO TO 860 865 IF (100 < 100) GO TO 865 870 IF (100 < 100) GO TO 870 875 IF (100 < 100) GO TO 875 880 IF (100 < 100) GO TO 880 885 IF (100 < 100) GO TO 885 890 IF (100 < 100) GO TO 890 895 IF (100 < 100) GO TO 895 900 IF (100 < 100) GO TO 900 905 IF (100 < 100) GO TO 905 910 IF (100 < 100) GO TO 910 915 IF (100 < 100) GO TO 915 920 IF (100 < 100) GO TO 920 925 IF (100 < 100) GO TO 925 930 IF (100 < 100) GO TO 930 935 IF (100 < 100) GO TO 935 940 IF (100 < 100) GO TO 940 945 IF (100 < 100) GO TO 945 950 IF (100 < 100) GO TO 950 955 IF (100 < 100) GO TO 955 960 IF (100 < 100) GO TO 960 965 IF (100 < 100) GO TO 965 970 IF (100 < 100) GO TO 970 975 IF (100 < 100) GO TO 975 980 IF (100 < 100) GO TO 980 985 IF (100 < 100) GO TO 985 990 IF (100 < 100) GO TO 990 995 IF (100 < 100) GO TO 995 1000 IF (100 < 100) GO TO 1000					

BEST AVAILABLE COPY

PROGRAM LINE	7/7/76	OPT=1	FTN 4.5-4006	10-22-76	PAGE
000	IVALEVEL=7				74224000
	GO TO 100				74224010
745	CONTINUE				74224020
C	IF (TIME(1,0)-600.0) GO TO 105				74224030
	IF (TIME(2,0)-1000.0) GO TO 240				74224040
405	GO TO 165				74224050
	WRITE(6,255)				74224060
255	FORMAT(9X, 'THE VEHICLE HAS TAKEN OFF.')				74224070
260	WRITE(6,260) (ZCUM(I),I=1)				74224080
262	FORMAT(13X, 'END OF SUMMARY. PFI0.0')				74224090
263	OPEN = 1				74224100
	PSWMS=0.				74224110
	CCWMS=0.				74224120
261	DO 263 I=1,MM				74224130
	CCWMS=CCWMS+CCACC(I)*0.2				74224140
266	DO 266 I=1,LL				74224150
	PSWMS=PSWMS+SACC(I)*0.2				74224160
	PSWMS=100.0-3247(PSWMS)/FLOAT(ILL)				74224170
	CCWMS=100.0-3247(CCWMS)/FLOAT(ILL)				74224180
746	WRITE(6,265) PSWMS,CCWMS				74224190
	FORMAT(17/23X, 'PSWMS=0.0, CCWMS=0.0, PFI0.0')				74224200
	IF (PFI0.0-0.0) GO TO 245				74224210
	ELONG = FLOAT(MCH)/5.				74224220
265	WRITE(6,265) WMLL				74224230
	FORMAT(22X)				74224240
	IF (WMLL-1000.0) GO TO 246				74224250
267	FORMAT(13X, 'THE ARRAYS CACC OR PSACC OR MCH 44WF ENTERED				74224260
	1 THEIR DIMENSIONED SIZE.')				74224270
268	CONTINUE				74224280
	CALL FACTOR (7.0)				74224290
	CALL PLT(10.0,-11.0,-5)				74224300
	CALL PLT(13.0,-7.0,-5)				74224310
435	TIME(MM+2) = 5.0				74224320
	TIME(ILL+1) = 5.0				74224330
	TIME(ILL+2) = 5.0				74224340
	CCACC(MM+1) = 1.0				74224350
	CCACC(MM+2) = 1.0				74224360
440	PSACC(ILL+1) = 1.0				74224370
	PSACC(ILL+2) = 1.0				74224380
	CALL SCALE(MM+10,MM+1)				74224390
	MM+10 = MM+10				74224400
445	IF (MM+10-0.0) GO TO 275				74224410
	MM+10 = MM+10				74224420
	IF (MM+10-0.0) GO TO 275				74224430
	MM+10 = MM+10				74224440
450	CALL ANTS(10.0,11.0,TIME(1),				74224450
	TIME(MM+2))				74224460
	ELONG = ELONG				74224470
	CALL PLT(10.0,11.0,1)				74224480
	CALL PLT(13.0,7.0,1)				74224490
455	CALL SYMOL (11.0,10.0,300) STANCE,0.0)				74224500
	CALL SYMOL (11.0,10.0,300) STANCE,0.0)				74224510
	DO 275 I=1,ELONG				74224520

● 中国文学名著丛书 9872

[illegible]

58

55

60

BEST AVAILABLE COPY

SUBROUTINE C0 - 76/74 OPT=1 PAGE 1

1 COUTINE C0FF (Y, 1, M, C, 0)

5 CENSION V(6)

6 V(1)

7 C (96.0*V(1)+96.0*V(2)-64.0*V(3)+4.0*V(4))/(-128.0)

8 C (-16.0*V(1)-12.0*V(2)+15.0*V(3)-4.0*V(4))/(-128.0)

9 RETURN

END

05/25/76 10.22.28

FTN 4.540406

C0FF0010

C0FF0020

C0FF0030

C0FF0040

C0FF0050

C0FF0060

C0FF0070

C0FF0080

SUBROUTINE TL00 - 76/74 OPT=1 PAGE 1

1 SURROUTINE TL00 (X, SLOPE, YCEPT, S, D, N)

5 DIMENSION S(10), P(10)

10 THIS IS A 2 DIMENSIONAL TABLE LOOK UP ROUTINE

15 WITH LINEAR INTERPOLATION

20 X IS THE CURRENT VALUE OF STROKE

25 SLOPE AND YCEPT ARE CALCULATED AND RETURNED

30 S AND D MAKE UP THE TABLE

35 N IS THE NUMBER OF VALUES IN THE TABLE

40 DO 1 I=1, N

45 IF (X-GE-S(I)) AND (X-LE-S(I+1)) GO TO 2

50 CONTINUE

55 SLOPE=(P(I+1)-P(I))/(S(I+1)-S(I))+.01

60 YCEPT=P(I)-SLOPE*S(I)

65 RETURN

END

05/25/76 10.22.28

FTN 4.540406

TL 0010

TL 0020

TL 0030

TL 0040

TL 0050

TL 0060

TL 0070

TL 0080

TL 0090

TL 0100

TL 0110

TL 0120

TL 0130

TL 0140

TL 0150

TL 0160

TL 0170

AFFDL-TR-77-37

APPENDIX C
LISTING OF AIRPLANE DATA

- Boeing 727-100
- McDonnell Douglas C-9A
- AMST

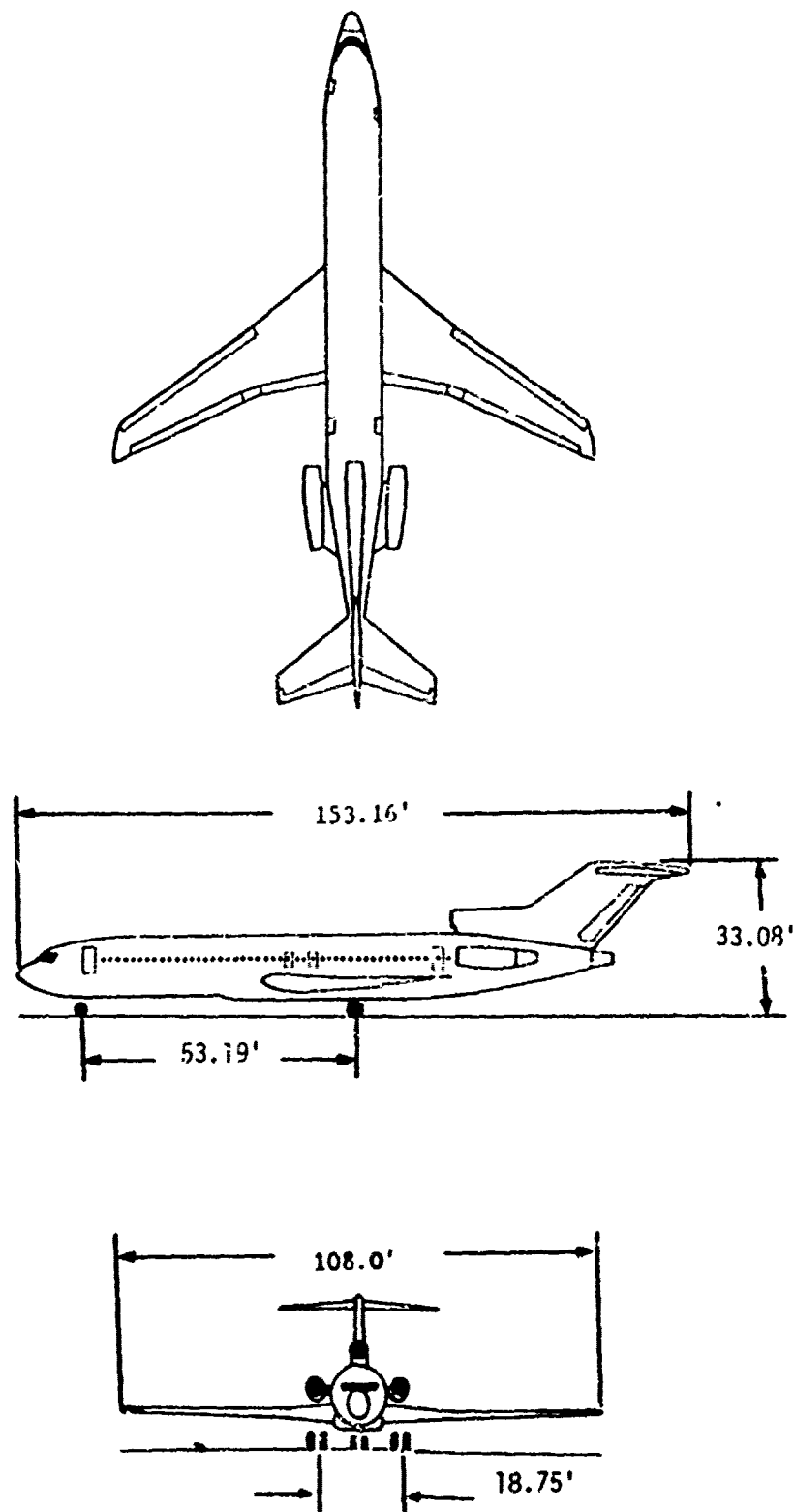


Figure C-1. Three View of Boeing 727-100

BEST AVAILABLE COPY

..... INP 7 DATA

..... GENERAL DISCREP DATA

301110 729-130 1447 17 0010005

W= 1461000	W= 131111	W= 695.0	A= 70.673	Q= 56P.703	MMIO 30453300.
S= 2.0	S= 1.7	SL= 112.1	SL= 134.0	PSAD= 645.9	TAILO= 211.1
AS= 53.26	AS= 43.9	AS= 293.1	W= 732.90	Q= 1.77	TS= 22740.04
AS= 19.0	AS= 14.1	AS= 251.0	VC= 221.90	Q= .95	TS= 4994.30
CL= .310	CL= .181	AS= 1940.0	AS= 50.0	TAUST= 11030.	TAOFF= 252.30

STRAKE NOSE 314 31400000

2.220	.374
2.440	.276
1.197	1.143
1.140	1.023
1.140	1.020
1.140	1.023

SINCE MAIN 314 31400000

2.220	1.050
1.140	1.111
1.140	1.193
1.140	1.003

BEST AVAILABLE COPY

MODE	SIPOS	SINOSF	SIGI	TIMEIN	STRAIL	OMEGA	GEN. MASS
1	-0.23	-0.23	-0.22	-0.33	-0.06	14.08	6.6
2	-0.25	-0.22	-0.14	-0.29	-0.06	22.97	7.0
3	-0.17	-0.14	-0.02	-0.00	-0.06	34.35	2.7
4	-0.23	-0.16	-0.11	-0.19	-0.02	44.55	11.3
5	-0.32	-0.21	-0.11	-0.11	-0.02	49.11	1.9
6	-0.21	-0.16	-0.10	-0.13	-0.04	54.66	3.0
7	-0.15	-0.14	-0.14	-0.14	-0.03	75.56	1.6
8	-0.13	-0.10	-0.12	-0.10	-0.06	82.63	171.9
9	-0.00	-0.13	-0.16	-0.05	-0.13	47.55	25.1
10	-0.05	-0.13	-0.14	-0.11	-0.10	9.74	11.5

..... INITIAL CONDITIONS

ZM0 -0.11; PM0 -1.475 IME0 -0.0575 ZOM0 -13.573
 TIME0 -17.800 POS0 -0.023 SICT0 -1614.0 PFAC0 -179851.

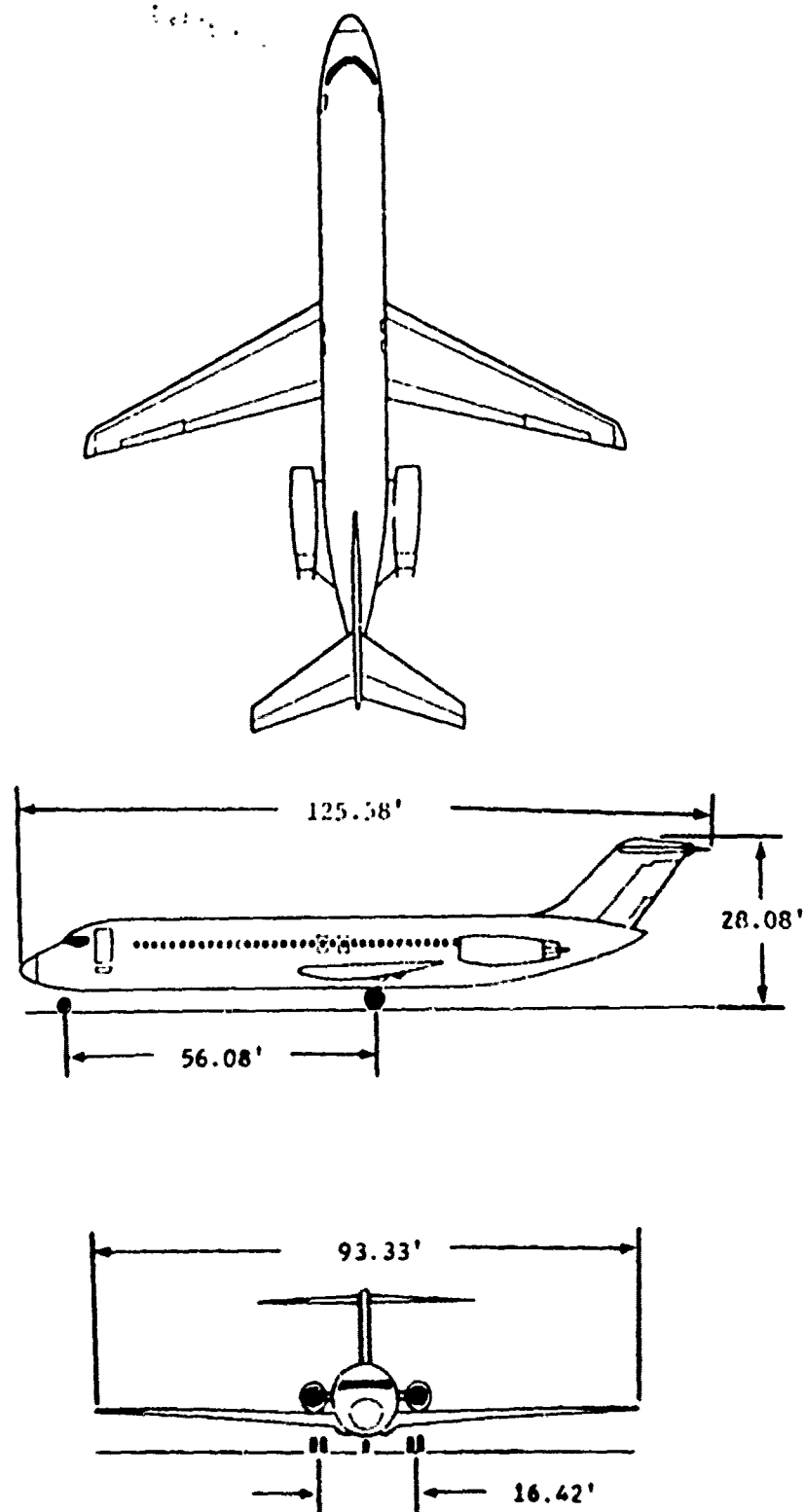


Figure C-2. Three View of McDonnell-Douglas C-9A

BEST AVAILABLE COPY

..... INPUT DATA

..... Aircraft Data

Case 1.0... 40.

NO	1.0...	WTS	527.14	MM	11.443	40	21.061	30	50.444	WTS	96.656	MM	26.0360.
WTS	1.0...												
3400	40.	5200	10.	5.000	00.5	21.00	07.5	0.5000	0.7.4	24.2000	310.5		
4400	11.00	4000	10.00	10.000	22.000	10.00	10.000	0.0000	0.000	150.00	23.000.67		
5100	0.80	4000	0.70	0.000	10.000	10.00	10.000	0.0000	0.000	10.00	0.000		
6100	1.00	0.00	0.00	0.000	1.000.7.	30	0	5.00	10.000	20.000	205.50		

STRUCTURE DATA

1.000	0.00
2.000	0.00
3.000	0.00
4.000	0.00
5.000	0.00

STRUCTURE DATA

1.000	0.00
2.000	0.00
3.000	0.00
4.000	0.00
5.000	0.00

BEST AVAILABLE COPY

1900	1905	1910	1915	1920	1925
1	100.5	100.5	100.5	100.5	100.5
2	100	100	100	100	100
3	100	100	100	100	100
4	100	100	100	100	100
5	100	100	100	100	100
6	100	100	100	100	100
7	100	100	100	100	100

MODE	SLIP	SLIP	SLIP
1	0	0	0
2	0	0	0
3	0	0	0
4	0	0	0
5	0	0	0
6	0	0	0
7	0	0	0
8	0	0	0
9	0	0	0
10	0	0	0
11	0	0	0
12	0	0	0
13	0	0	0
14	0	0	0
15	0	0	0
16	0	0	0
17	0	0	0
18	0	0	0
19	0	0	0
20	0	0	0
21	0	0	0
22	0	0	0
23	0	0	0
24	0	0	0
25	0	0	0
26	0	0	0
27	0	0	0
28	0	0	0
29	0	0	0
30	0	0	0
31	0	0	0
32	0	0	0
33	0	0	0
34	0	0	0
35	0	0	0
36	0	0	0
37	0	0	0
38	0	0	0
39	0	0	0
40	0	0	0
41	0	0	0
42	0	0	0
43	0	0	0
44	0	0	0
45	0	0	0
46	0	0	0
47	0	0	0
48	0	0	0
49	0	0	0
50	0	0	0
51	0	0	0
52	0	0	0
53	0	0	0
54	0	0	0
55	0	0	0
56	0	0	0
57	0	0	0
58	0	0	0
59	0	0	0
60	0	0	0
61	0	0	0
62	0	0	0
63	0	0	0
64	0	0	0
65	0	0	0
66	0	0	0
67	0	0	0
68	0	0	0
69	0	0	0
70	0	0	0
71	0	0	0
72	0	0	0
73	0	0	0
74	0	0	0
75	0	0	0
76	0	0	0
77	0	0	0
78	0	0	0
79	0	0	0
80	0	0	0
81	0	0	0
82	0	0	0
83	0	0	0
84	0	0	0
85	0	0	0
86	0	0	0
87	0	0	0
88	0	0	0
89	0	0	0
90	0	0	0
91	0	0	0
92	0	0	0
93	0	0	0
94	0	0	0
95	0	0	0
96	0	0	0
97	0	0	0
98	0	0	0
99	0	0	0
100	0	0	0

```

***** 1414 CONDITIONS *****
ZMS  -0.113  ZMS  -0.113  TMS1414  -0.113  26614  -17.21-31146.
END1414  -0.113  END1414  -0.113  END1414  -0.113  -99316.

```

69

[illegible]

APPENDIX D
LISTING OF RUNWAY PROFILES

1. Figure D-1 - Washington National Runway 36-Left, Center, and Right hand profiles:
2. Profile data listing of the 1-cos dip used in these simulations:
All three lines of profile were identical except that they occur at different times corresponding to the gear locations.

Figure D-1. Washington National Runway 36 with Linear Trand Removed

BEST AVAILABLE COPY

100-443887-100

BIBLIOGRAPHY

Butterworth, C. K., and Boozer, D. E., Jr., C-141A Computer Code for Runway Roughness Studies, AFWL-TR-70-71, Air Force Weapons Laboratory, Kirtland AFB, New Mexico, August 1970.

Chance Vought Corporation, A Rational Method for Predicting Alighting Gear Dynamic Loads, ASD-TDR-62-555, Aeronautical Systems Division, Wright-Patterson AFB, Ohio, December 1963.

Cook, Robert F., Use of Discrete Runway Profile Elevation Data in Determining the Dynamic Response of Vehicles, TM-68-3-FDDS, Air Force Flight Dynamics Laboratory, Wright-Patterson AFB, Ohio, May 1968.

Crenshaw, B. M., and Butterworth, C. K., Lockheed Georgia Company, Aircraft Landing Gear Dynamic Loads from Operation on Clay and Sandy Soil, AFFDL-TR-69-51, Air Force Flight Dynamics Laboratory, Wright-Patterson AFB, Ohio, February 1971.

NACA TN 2477, Investigation of the Air-Compression Process During Drop Tests of an Oleo-Pneumatic Landing Gear, 1951.

Quade, Delmar A., The Boeing Company, Wichita Division, Location of Rough Areas of Runways for B-52 Aircraft, AFFDL-TR-67-175, Air Force Flight Dynamics Laboratory, Wright-Patterson AFB, Ohio, March 1968.

REFERENCES

1. Goldman, D. E., and von Gierke, H. E., 'Effects of Shock and Vibration on Man,' Volume III, Chap. 44, Shock and Vibration Handbook (C. M. Harris and C. E. Crede, editors) McGraw Hill Book Co., New York, 1961.
2. Gerardi, A. G., Lohwasser, A. K., Computer Program for the Prediction of Aircraft Response to Runway Roughness, AFWL-TR-73-109, Volume I and II, Air Force Weapons Laboratory, Kirtland AFB, New Mexico, September 1973.